Gondwana Research 23 (2013) 1491–1510

Contents lists available at SciVerse ScienceDirect

Gondwana Research

journal homepage: www.elsevier.com/locate/gr

Documenting basin scale, geometry and provenance through detrital geochemical data: Lessons from the Neoproterozoic to Ordovician Lesser, Greater, and Tethyan Himalayan strata of Bhutan

N. McQuarrie [a,*], S.P. Long [b], T. Tobgay [c], J.N. Nesbit [c], G. Gehrels [d], M.N. Ducea [d,e]

[a] Department of Geology and Planetary Sciences, University of Pittsburgh, United States
[b] Nevada Bureau of Mines and Geology, University of Nevada, Reno United States
[c] Department of Geosciences, Princeton University, United States
[d] Department of Geosciences, University of Arizona, United States
[e] Universitatea Bucuresti, Facultatea de Geologie si Geofizica, Bucuresti, 010041 Romania

ARTICLE INFO

Article history:
Received 30 January 2012
Received in revised form 8 September 2012
Accepted 27 September 2012
Available online 6 October 2012

Handling Editor: M. Santosh

Keywords:
Detrital zircon
Himalaya
Bhutan
Isotopes
Indian margin

ABSTRACT

Detrital zircon (DZ) ages, augmented with εNd(0) and $\delta^{13}C$ isotopic values from 18 new and 22 published samples collected from Lesser Himalayan (LH), Greater Himalayan (GH) and Tethyan Himalayan (TH) rocks in Bhutan, support deposition of >7 km of sedimentary rock in late Cambrian–Ordovician time and provide a stratigraphic framework for the pre-collisional Indian margin. Youngest GH DZ grains become younger upsection from 900 Ma to 477 Ma. Youngest DZ grains in TH samples are ~490–460 Ma. Both the LH Jaishidanda Formation (Fm), and the LH Baxa Group overlie Paleoproterozoic LH rocks. The Jaishidanda Fm exhibits distinct populations of youngest DZ peaks, 475–550 Ma, and 800–1000 Ma. The Baxa Group (Manas, Pangsari, and Phuntsholing formations) contains youngest DZ peaks at both 500–525 Ma and 0.9–1.0 Ga. However, most samples from the Baxa Group in western Bhutan contain no grains younger than 1.8 Ga. Samples from the LH Paro Fm, which sits directly under the MCT in western Bhutan, have youngest DZ peaks at 0.5, 0.8, 1.0, 1.7, 1.8 Ga. εNd values generally match DZ spectra, with samples that contain old, youngest grain populations corresponding to more negative εNd signatures. The Paro Fm is an exception where εNd (0) values from quartzite samples are quite negative (−19 to −24) whereas the εNd (0) values from interbedded schist contain younger detritus (−12 to −17). $\delta^{13}C$ values from the Jaishidanda, Paro and Manas formations have $\delta^{13}C$ values (−1.8 to +6) suggestive of deposition over late Neoproterozoic to Ordovician time. $\delta^{13}C$ values from the Pangsari Fm vary from −2.8 to +1.8, compatible with deposition in the early- to middle Neoproterozoic. The young, latest Cambrian–Ordovician grains preserved in TH, GH and LH rocks suggest that the late Cambrian–Ordovician orogeny, documented in GH rocks throughout the orogen, served as a significant sediment source in Bhutan.

1. Introduction

In orogenic belts such as the Himalaya, where much of the original sedimentary package has been significantly metamorphosed, deriving the original stratigraphy and geometry of the pre-collisional sedimentary basin is challenging, but fundamentally important. Although subject to uncertainties in depositional age, source area and basin extent, the task of documenting the original stratigraphic architecture of an orogen is critical because the geometry, thickness and lateral continuity of sedimentary basins exert a first-order control on fold-thrust belt structures and deformation geometry (e.g., Mitra, 1994; McQuarrie, 2004; Mitra et al., 2010; Long et al., 2011a, 2011b). The vertical distribution of rock types exerts the strongest control on the locations of weak decollement horizons, which fundamentally control the large-scale dimensions of an orogenic belt (i.e., critical taper) (Davis et al., 1983; Dahlen and Suppe, 1988; Dahlen, 1990). Lateral variations in basin geometry (and therefore, initial taper) as well as lateral variations in strength and distribution of weak stratigraphic horizons may result in different thrust offset magnitude, different thrust geometries, and distinct structural styles both along and across strike in a thrust belt (Mitra, 1994; McQuarrie, 2004). Correlations of stratigraphy and structures along-strike are interrelated and critical in this process. An understanding of the stratigraphy, geometry, and spatial variations of pre-deformational basins can also result in definition of overlap sequences that can greatly aid in differentiating deformation timing and extent in polymetamorphic rocks. Thus, correctly identifying these basin parameters is essential to understanding an orogen at both local and regional scales.

In the Himalayan orogen, documenting the location and distribution of Neoproterozoic through Ordovician deposits can provide insight into the extent, nature and magnitude of pre-Himalayan deformation, the potential for significant lateral variations within the original margin

* Corresponding author.
E-mail addresses: nmcq@pitt.edu (N. McQuarrie), splong@unr.edu (S.P. Long), ttobgay@princeton.edu (T. Tobgay), jnesbit@Princeton.edu (J.N. Nesbit), ggehrels@email.arizona.edu (G. Gehrels), ducea@email.arizona.edu (M.N. Ducea).

1342-937X/$ – see front matter
http://dx.doi.org/10.1016/j.gr.2012.09.002

architecture, and the control regional basins exerted on the location and deformation path of modern Himalayan structures. In this manuscript we present detrital zircon (DZ) ages augmented with both whole-rock Nd and $\delta^{13}C$ isotopic values from 18 new and 22 published samples collected from LH, GH and TH rocks in the eastern Himalayan kingdom of Bhutan. From this data we can argue for Neoproterozoic through Ordovician deposition in rocks interpreted as belonging to the LH, GH and TH zones. Although our data show that all three tectonostratigraphic zones experienced deposition over this time window, there is significant variation in provenance expressed as DZ spectra and εNd values. We suggest that this variation is a function of proximity to source regions, locations of major rivers, and basin scale geometry. This provides insight into larger, margin-wide deposition over this time window that is critical for constructing pre-Himalayan stratigraphic architecture.

2. Himalayan background

The ongoing collision between India and Asia, which began ca. 60–55 Ma (LeFort, 1975; Klootwijk et al., 1992; Rowley, 1996; Hodges, 2000; Guillot et al., 2003; DeCelles et al., 2004; Leech et al., 2005), has deformed the original sedimentary cover that blanketed the northern Indian craton, thereby constructing the Himalayan orogenic belt. Throughout Cenozoic time, India has moved northward with respect to Asia, and as a result, large, south-vergent thrust sheets have buried, metamorphosed and then displaced the original basin stratigraphy. Since they are now deformed and translated to the south along their entire east–west length, many questions remain regarding the spatial and temporal architecture of the original, composite sedimentary basin (e.g., Brookfield, 1993; Valdiya, 1995; Parrish and Hodges, 1996; DeCelles et al., 2000; Gehrels et al., 2003; Myrow et al., 2003; Yin, 2006; Myrow et al., 2010). The problem is further compounded because the Himalayan tectonostratigraphic packages were originally defined by the relationships of rocks to orogen-scale structures such as the Main Central thrust, which is recognized along the full length of the orogen (Gansser, 1964; LeFort, 1975; Hodges, 2000; Yin, 2006). These major structures were originally identified based on significant changes in metamorphic grade, such as abrupt juxtaposition of higher-grade rocks over lower-grade rocks (Heim and Gansser, 1939; Gansser, 1964; LeFort, 1975). From south to north, the classic tectonostratigraphic subdivisions and major bounding faults are the Indo-Gangetic foreland basin, the Main Frontal thrust, the Subhimalayan zone, the Main Boundary thrust (MBT), the Lesser Himalayan (LH) zone, the Main Central thrust (MCT), the Greater Himalayan (GH) zone, the South Tibetan detachment system (STDS), the Tethyan Himalayan (TH) zone, and the Indus-Yalu suture zone, which marks the northern limit of rocks associated with India (Fig. 1).

Geochemical signatures from DZ and/or εNd of LH, GH, and TH strata have been used to define stratigraphic horizons, help identify important geologic structures, and determine unroofing histories (e.g., Parrish and Hodges, 1996; Robinson et al., 2001; DeCelles et al., 2004; Martin et al., 2005; Richards et al., 2005, 2006; Imayama and Arita, 2008; McQuarrie et al., 2008; Myrow et al., 2009, 2010; Tobgay et al., 2010; Long et al., 2011a; Webb et al., 2011; Spencer et al., 2012). These lithotectonic units record the pre-collisional geologic history of the greater Indian margin, and the geochemical datasets mentioned above, combined with stratigraphic and structural relationships observed in the field, allow us to reconstruct their original basin architecture.

3. Bhutan tectonostratigraphy

We highlight the critical data on lithologic characteristics, DZ ages, εNd(0) values and $\delta^{13}C$ isotopic ratios for major formations in the Bhutan Himalaya in Table 1. The formations are organized with respect to their main tectonostratigraphic zones (TH, GH, LH) from north to south (Fig. 2). Studies in the Bhutan Himalaya have highlighted important variations to the simplified Himalayan tectonostratigraphy outlined in Section 2. The most critical of these is the definition of the TH. While in many places the TH is separated from the GH by a large top-to the north shear zone (Burchfiel et al., 1992; Grujic et al., 2002; Webb et al., 2007), Long and McQuarrie (2010) argued that in Central Bhutan, that shear zone is either missing, or broadly distributed through a 10 km section of both GH and TH rocks. Because of the lack of a distinct bounding structure, they defined the GH–TH contact at the base of the clean, cliff forming quartzite of the Chekha Formation (Gansser, 1983; Long and McQuarrie, 2010) that is typically in the immediate hanging wall of mapped portions of the STDS through Bhutan (Grujic et al., 2002) and we follow that definition in this paper. Also unique to Bhutan is the occurrence of GH rocks over a significant portion of the Bhutan landscape. Grujic et al. (2002) divided the Bhutan GH section into a lower structural level above the MCT and below a younger, out-of-sequence structure, the Kakhtang thrust (KT), and a higher structural level above the KT (Fig. 1). The higher structural section contains the bulk of leucogranite exposed in Bhutan (Gansser, 1983; Swapp and Hollister, 1991; Davidson et al., 1997). Our discussion of GH rocks is completely focused on the lower structural level between the MCT and the KT. Following Gehrels et al. (2011), the LH strata above the MBT and below the MCT are divided into a lower LH section composed of Paleoproterozoic age strata while Neoproterozoic and younger LH strata are grouped in an upper LH section (Table 1).

4. Methods

4.1. U–Pb geochronology

U–Pb geochronologic analyses were conducted on individual grains using laser-ablation multicollector inductively coupled plasma mass spectrometry (LA-MC-ICP-MS) at the University of Arizona LaserChron Center (Gehrels et al., 2006b, 2008) (Appendix 1). Approximately 100 grains were dated per sample, although for samples that did not contain 100 dateable grains, all available zircons were analyzed. Low zircon yields were common for Baxa Group rocks in western Bhutan (BU10-93, BU10-73, and BU10-64). We analyzed two TH samples, seven samples from the GH section (Fig. 1) and nine samples from the LH Baxa Group (Fig. 3, Tables 1, 2). The seven GH samples were selected so that when combined with previously published samples, the data cover a broad geographical area as well as provide data from the base to the top of the section. The TH samples were collected from Chekha Formation quartzite immediately above the STDS. For the LH samples, we focused our sampling in western Bhutan to complement published data from eastern Bhutan (McQuarrie et al., 2008; Long et al., 2011a). In particular, we sampled the coarsest quartzite beds in the Pangsari and Phuentsholing formations, as well as a range of beds in the Manas/Jainti Formation.

Reported uncertainties for individual analyses are at the 1σ level (Appendix 1). In general, $^{206}Pb^*/^{238}U$ ratios were used for ages younger than 1.0 Ga, and $^{207}Pb^*/^{206}Pb^*$ ratios were used for ages older than 1.0 Ga (asterisk denotes correction for common Pb; all ages described in the text have had this correction). Other possible sources of error, in addition to instrument errors (Appendix 1), include uncertainties in U decay constants, common Pb composition, and calibration to the zircon standard used. These errors could shift the age-probability peaks by up to ~3% (2σ). These external uncertainties provide a minimum uncertainty on sets of ages (e.g., a peak on an age-distribution diagram). Analyses that are >30% discordant (by comparison of 206Pb/238U and 206Pb/207Pb ages) or >5% reverse discordant were not considered further. Acceptance of analyses with up to 30% discordance allows us to include most of the age information from each sample, and therefore yields a more complete and accurate description of provenance components. After a general 30% discordancy filter was applied, a few GH samples displayed a population of young ages that are pulled off of concordia and project to an

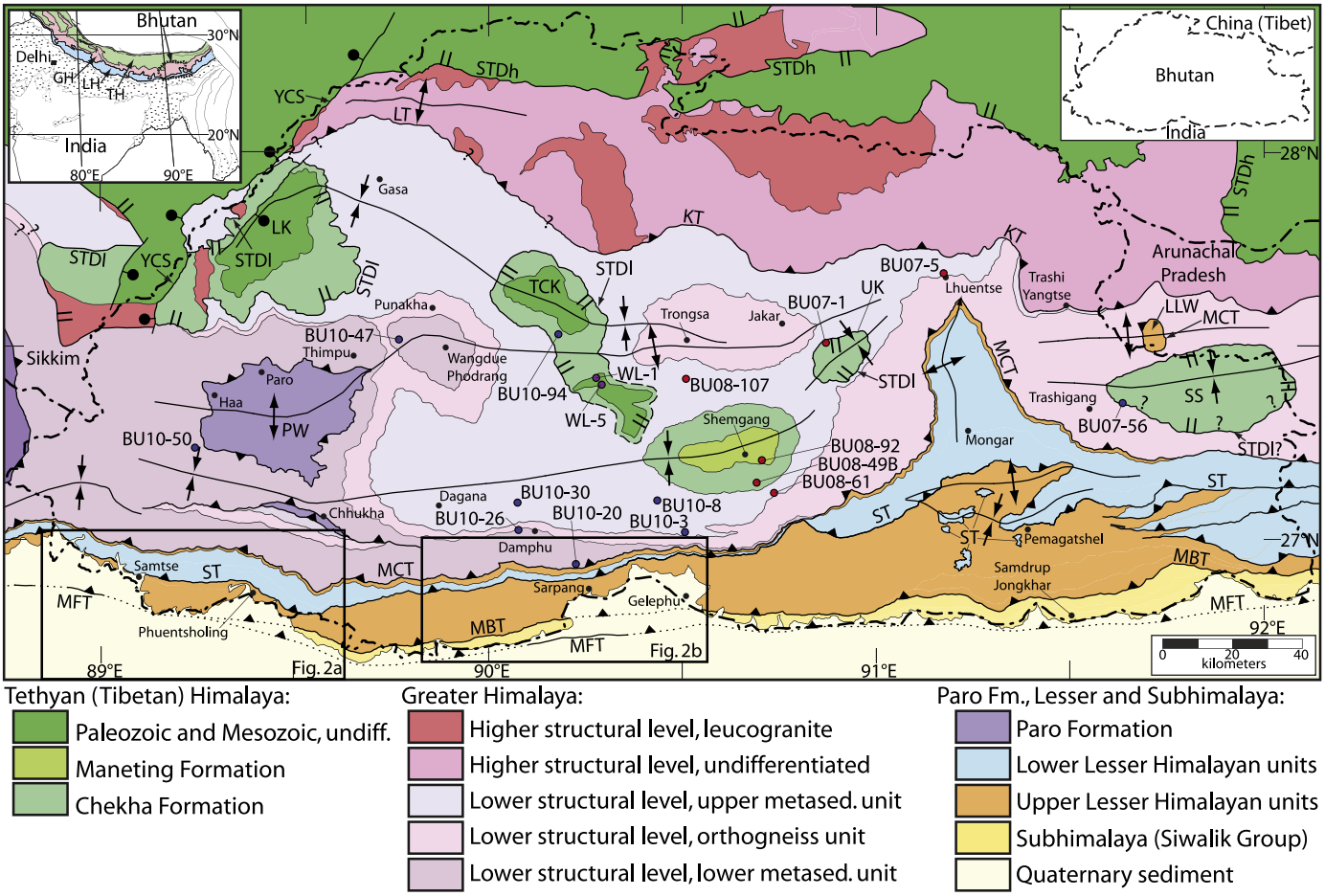

Fig. 1. Geologic map of Bhutan and surrounding region, simplified from Long et al. (2011c). Areas of detailed geologic maps in Fig. 3 are shown. Upper left inset shows generalized geologic map of central and eastern Himalayan orogen (modified from Gansser, 1983). Abbreviations: 1) inset: GH: Greater Himalaya, LH: Lesser Himalaya, TH: Tethyan Himalaya: 2) structures from north to south: YCS: Yadong Cross-Structure, STDh: structurally-higher South Tibetan Detachment, LT: Laya Thrust (location from Chakungal et al., 2010), KT: Kakhtang Thrust, STDl: structurally-lower South Tibetan Detachment, MCT: Main Central Thrust, MBT: Main Boundary Thrust, MFT: Main Frontal Thrust; 3) windows and klippen from west to east: LK: Lingshi Klippe, PW: Paro Window, TCK: Tang Chu Klippe, UK: Ura Klippe, SS: Sakteng syncline, LLW: Lum La Window (location from Yin et al., 2010b).

upper intercept age of ~20 Ma. In these cases, the young, discordant ages along this trend are also removed and not plotted on the relative age-probability diagrams (Appendix 1). The resulting interpreted ages are shown on age-distribution (relative age-probability) diagrams, which are a sum of probability distributions for all analyses from a sample (Figs. 4 and 5).

Maximum depositional ages are reported for some strata using the youngest single grain, with the qualifier that a single grain may yield a maximum depositional age that may be younger than the true depositional age due to Pb-loss or simply due to measurement statistics (Dickinson and Gehrels, 2009). This was done generally for samples with low zircon yield. For most samples we use the more robust criteria of using the youngest statistically significant peak in age probability, which is defined by at least three analyses that overlap within error.

4.2. Epsilon Neodymium isotope geochemistry

Nd isotopic ratios and the elemental concentrations of Sm and Nd were measured by thermal ionization mass spectrometry at the University of Arizona, following procedures reported by Otamendi et al. (2009) (Appendix 2). Analyses were performed on five Baxa Group phyllite samples, two from the Pangsari Formation and three from the Phuentsholing Formation to compare with previously published analyses. For each sample, the average of 100 isotopic ratios was taken to calculate the εNd value. Analyzed samples have estimated analytical $\pm 2\sigma$ uncertainties of $^{147}Sm/^{144}Nd = 0.4\%$, and $^{143}Nd/^{144}Nd = 0.0012\%$, which corresponds to an εNd error of ±0.5 (Table 3). We report Nd isotopic composition using εNd(0) values. This is a common practice for Himalayan rocks and it facilitates comparison to previous analyses in Bhutan and along the Himalayan arc.

4.3. Carbonate C and O isotope measurement

Samples were collected for carbon and oxygen isotope analysis from six stratigraphic sections of dolostone from the Phuentsholing and Pangsari formations of the Baxa Group, two stratigraphic sections within the marble bands of the Paro Formation and one marble section from the Jaishidanda Formation (Table 2) (Figs. 1, 3). Wide sample spacing, combined with the limited thickness of carbonate beds within the formations precludes matching specific isotopic trends, or plotting isotopes on stratigraphic columns. Instead our goal is to determine the general isotopic values, specifically looking for high positive $\delta^{13}C$ values in our data that may be matched to periods of time with similar positive excursions. Meteoric diagenesis, diagenetic reprecipitation of organic carbon, and alteration through metamorphism are the most likely ways to modify the absolute values of $\delta^{13}C$ after deposition. These processes tend to shift absolute values more negative, not more positive (Allan and Matthews, 1982; Lohmann, 1988; Kaufman and Knoll, 1995; Guerrera et al., 1997; Jacobsen and Kaufman, 1999; Melezhik et al., 2003; Knauth and Kennedy, 2009). Phuentsholing Formation samples SBU 1, SBU 2, and SBU 4 are single samples from individual

Table 1
Summary of critical data on lithologic characteristics, DZ ages, εNd(0) values and δ13C isotopic ratios for major formations in the Bhutan Himalaya.

Tectonostratigraphic zone	Formation	Youngest DZ peak	Prominent DZ peaks	εNd (0)[a]	δ13C	Independent age constraints	Prominent lithologies	Documented stratigraphic contacts	Section thickness
Tethyan Himalaya									
–Shemgang region (and locales to the east, Ura and Sakteng)	Chekha Formation	488–460 Ma (1,2)	490, 600 Ma, 1.2, 1.6–1.7 Ga				Tan to white, fine- to medium-grained, cliff-forming, locally conglomeratic quartzite. 5–10% muscovite and biotite, and rare garnet porphyroblasts (1,2)	Long and McQuarrie (1) propose that the original contact between the Chekha and GH is depositional and is exposed in the Shemgang region, Bhutan.	2.2–3.5 km
	Maneting Formation						Dark-gray, graphitic, biotite-garnet phyllite (1,3).		1 km
–Tang Chug region	Chekha Formation	514 Ma (2)	490, 600 Ma, 1.2, 1.6–1.7 Ga				Thin- to medium-bedded basal quartzite, with common interbeds of fine-grained quartzite, thin schist layers, and green to white, thin-bedded marble (2)		2 km total
	Deshichiling Formation	494 Ma (4)	495, 600 Ma, 1.2, 1.6–1.7 Ga				Gray to brown, fine-grained quartz sandstone (4)		
	Maneting Formation						Unmetamorphosed sandstone, shale and carbonate (4,5) dark-gray shale		
	Quartzite Formation	500 Ma (4)	500, 600 Ma, 1.2, 1.6–1.7 Ga			Latest Cambrian, 494 Ma (4)	Gray, fine-grained sandstone		
	Wachi La–Ripakha Fms					Silurian (?)–Devonian (3)	Limestones, shales and dolostones (3,4)		
–Lingshi region	Chekha Formation						Tan, cliff-forming marble, with less abundant gray phyllite and dark-gray phyllitic quartzite (2, 5)		8 km total
	Additional units not specifically identified as formations in Gannser (5)					Devonian (3)	Medium-gray, cliff-forming, thin-bedded, fossiliferous limestone (3,5,6)		
						Permo-Carboniferous (5)	Diamictite		
						Mesozoic (5)	Dark-gray, tan weathering shale, fine-grained sandstone, dark-gray carbonaceous shale and brown sandstone		
Greater Himalaya									
	Lower metasedimentary unit	724 and 974 Ma (2)	700, 900 Ma, 1.0, 1.7 and 2.5 Ga	−12 to −17.5 (8)		Cambrian–Ordovician intrusions	Upper amphibolite to granulite-facies paragneiss with rare quartzite layers. 6.5–7 km in western Bhutan, a few 100 m in central Bhutan (1,6)	The lower metasedimentary unit of the GH section is intruded by late Cambrian–Ordovician age (480–500 Ma) plutons (1,6)	100 m to 7 km
	Orthogneiss	487 ± 7 Ma U–ePb (zircon) (1)				Cambrian–Ordovician	Orthogneiss, 1.5 km thick in western Bhutan, < 5 km in eastern Bhutan.		1.5-5 km

	Upper metasedimentary unit	477–460 Ma (1,2)	460, 500, 900 and 1000 Ma				Medium- to thick-bedded, micaceous quartzite interlayered with paragneiss and schist (1,6)		
Lower Lesser Himalaya									
	Shumar Formation	1816 ± 49 (7)	1.8–2.0, 2.5 Ga				Light-gray to light-green to white, fine-grained, medium- to thick-bedded quartzite that commonly forms massive cliffs (7)	Gradational depositional contact with Daling Fm over tens of meters of stratigraphic thickness (7,8)	1–6 km
	Daling Formation	1865 ± 47 (7)	1.8–2.0, 2.5 Ga	−25.9 to −32.3 (8,9)		1844 ± 64 Ma U–Pb crystallization age of granitic intrusions (7)	Green schist and phyllite with orthogneiss intrusions (7)	Intrusive contacts between phyllite and orthogneiss (7)	2–3 km
Upper Lesser Himalaya									
	Jaishidanda Formation	475–530 Ma (3 samples) and 0.8–1.0 Ga (5 samples) (7)	0.8, 1.0, 1.3, 1.7 Ga	−16.6 to −21.4 (8,9,10)	+2.4‰ to +6.5‰ (2)		Biotite-rich, locally garnet-bearing schist with interbedded biotite-laminated quartzite, and uncommon marble bands	Transition from Daling Formation to Jaishidanda Formation is marked by a distinct stratigraphic compositional change in quartzite, defined by an increase in the amount of biotite and lithic clasts	0.6–1.7 km
	Paro Formation	500 Ma	500, 600, 800 Ma, 1.0 1.2, 1.7, 1.8 Ga	Quartzite −18 to −24; schist −16 to −12	−2.9‰ to +3.7‰ (2)	450 Ma U–Pb crystallization age of granitic intrusions (10)	1–2 km-thick packages of fine-grained, thin-medium bedded quartzite separated by 10 –200 m-thick marble bands that are mappable across the entire exposure (10)		5 km
	Manas Formation (Baxa Group)	520 and 525 Ma	older peaks between 1.0 and 1.7 Ga	−21 (9)	+3‰ to +6‰ (7)		Fine to medium grained, locally pebbly to conglomeratic quartzite interbedded with phyllite and dolomite; the only Baxa Group formation exposed across the full east–west extent of Bhutan (6)	Depositional contacts between the Manas Formation and the underlying Daling Formation are observed in eastern most Bhutan (2).	2–3 km
	Jainti Formation	(Baxa 500 Ma)	older peaks between 1.0 and 1.7 Ga				Contains the same siliciclastic lithologies as the Manas Formation; however the Jainti Formation quartzite and phyllite are red to maroon. We combine both formations in the Manas Formation (6)		2–3 km
	Phuentsholing Formation (Baxa Group)	1.8 Ga	1.8–2.0 Ga	−24 to −26 (2)	−1.1‰, +1.8‰ (2)		Dark gray to black slate and phyllite with thin (10s of cm) interbeds of limestone, cream colored dolomite, and thin beds of dark-brown, fine-medium grained quartzite (12) only exposed in southwest Bhutan	The Manas Formation is mapped as a depositional contact below the Phuentsholing Formation in southwest Bhutan (6)	~2 km
	Pangsari Formation (Baxa Group)	1.7 Ga	1.7, 1.8–1.9, 2.15, 2.5 Ga	−27 (2)	−2.8‰ to +1.3‰ (2)		Dark-green to dark-gray, thin-bedded to laminated, locally talcose phyllite interbedded with white, pink, and green, medium- to thick-bedded dolostone and marble, and green, fine- to medium-grained, thin-bedded quartzite (12) only exposed in southwest Bhutan	Depositional contacts between the Buxa Formation (Pangsari equivalent) and the underlying Daling Formation are observed in Sikkim (11).	2.4 km
	Diuri Formation	390 Ma	390, 480, 800 Ma	−19.8 (9)			Dark-gray to green-gray, matrix-supported diamictite, with a micaceous slate matrix; abundant slate interbeds (7)	The Diuri Formation is mapped in depositional contact above the Manas Formation (7).	2–3 km
	Gondwana succession	500 Ma	500, 800 Ma, 1.2 Ga			Permian fish fossils (13)	Gray, medium-grained, poorly sorted, friable, feldspathic, lithic-rich sandstone, interbedded with dark-gray, thin- to medium-bedded, carbonaceous siltstone and shale (7)		0 to 2.4 km

References: (1) Long and McQuarrie, 2010; (2) This study; (3) Tangri and Pande, 1995; (4) Hughes et al., 2010; (5) Gansser, 1983; (6) Long et al., 2011d; (7) Long et al., 2011a; (8) Richard et al., 2006; (9) McQuarrie et al., 2008; (10) Tobgay et al., 2010; (11) Bhattacharyya and Mitra, 2009; (12) Tangri, 1995; (13) Joshi, 1989.

[a] Pubished εNd(500) values of GH rocks across Bhutan, were recalculated as εNd(0) values.

limestone and dolostone beds separated stratigraphically by several 100s of meters. SBU 1 is towards the middle of the section while SBU 2 is near the top of the Phuentsholing Formation (Fig. 3). SBU 4 is from the Phuentsholing Formation ~10 km to the west of SBU 1 and SBU 2. Phuentsholing Formation samples BU10-67 are from a ~15 m-thick dolomite bed near the middle of the section. For this section the stratigraphic spacing between samples is ~1 m. We sampled two dolomite sections in the Pangsari Formation. SBU 3 samples were taken over a 52 m stratigraphic distance. However, sample spacing is irregular due to variable thickness of interbedded phyllite. Samples were taken from discontinuous dolomite beds at intervals of less than 1 m to 4 m, depending on bed thickness, for a total of 14 samples. BU10-70 samples were taken every two meters from an ~80 m thick section of dolostone interbedded with quartzite. BU10-15 samples were taken every 2 m from a ~16 m-thick marble bed within the Jaishidanda Formation in south-central Bhutan (Fig. 3B). Samples were taken every ~2 m. Samples SBU 5 and SBU 6 are from marble bands within the Paro Formation. SBU 5 contains six samples collected every 1 m through the ~6 m thick marble band II, while seven SBU 6 samples were collected every 4 m through marble band I (Tobgay et al., 2010).

All samples were slabbed, polished and then micro-drilled to collect 5 mg of powder for isotopic analysis. The most pristine carbonate was targeted, and care was taken to avoid cements and secondary veins or precipitates. All powders were heated to 110 °C to remove water. Samples were prepared at Princeton University and analyzed at Princeton University and the University of Rochester. At both universities the $\delta^{13}C$ and $\delta^{18}O$ values were measured simultaneously on an automated carbonate preparation device (Gasbench II) coupled directly to the inlet of a Thermo DeltaPlus continuous flow isotope ratio mass spectrometer. Data are reported in permil (‰) notation relative to VPDB (Vienna Pee Dee Belemnite). Final $\delta^{13}C$ values were averaged for each sample (Appendix 3) (Fig. 6).

5. Results

5.1. U–Pb geochronology

We analyzed two TH samples, both collected from the Chekha Formation in the immediate hanging wall of the STDS. BU10-94 was collected in the Tang Chu klippe (Fig. 1). Although the number of analyzed DZ grains was limited (n = 35), BU10-94 shows pronounced peaks at 514, 650, and 1095 Ma. BU07-56 was collected in the Sakteng syncline, and displays peaks at 488, 992 and 1096 Ma (Fig. 4).

We analyzed seven GH samples in this study. BU10-20 was collected from the base of the GH section (lower metasedimentary unit) immediately above the MCT in south-central Bhutan (Fig. 1). BU10-20 has a significant peak at 970 Ma and smaller peaks at 1597, 1697, and 2496 Ma. Samples BU10-50 and BU10-47 were also collected from the lower metasedimentary unit in western Bhutan (Fig. 1). BU10-50 has a similar DZ age spectra to BU10-20, with the addition of younger peaks at 724 and 824 Ma, whereas BU10-47 displays only Paleoproterozoic peaks at 1.8, 1.95, and 2.48 Ga. BU10-26 was collected in the uppermost part of the lower metasedimentary unit, immediately below the orthogneiss unit in south-central Bhutan (Fig. 1). BU10-26 yielded a similar DZ age spectra to BU10-50 and BU10-20, with youngest peaks at 812 and 974 Ma. BU10-30, BU10-8 and BU10-3 were all collected from the upper GH metasedimentary unit. Both BU10-8 and BU10-3 have youngest peaks at 477 Ma, with older significant peaks at 815, 940 and 1050 Ma. BU10-30 contains older peaks at 750 and 960 Ma, but lacks the young Ordovician grains that characterize the other upper metasedimentary unit samples (Fig. 4).

Nine new samples were analyzed from the Baxa Group in western and central Bhutan. Samples BU10-89 and BU10-64 were collected from the Manas Formation. BU10-89 yielded a youngest large peak at 1.87 Ga, with a series of older peaks through 2.5 Ga. BU10-64 has a wider range

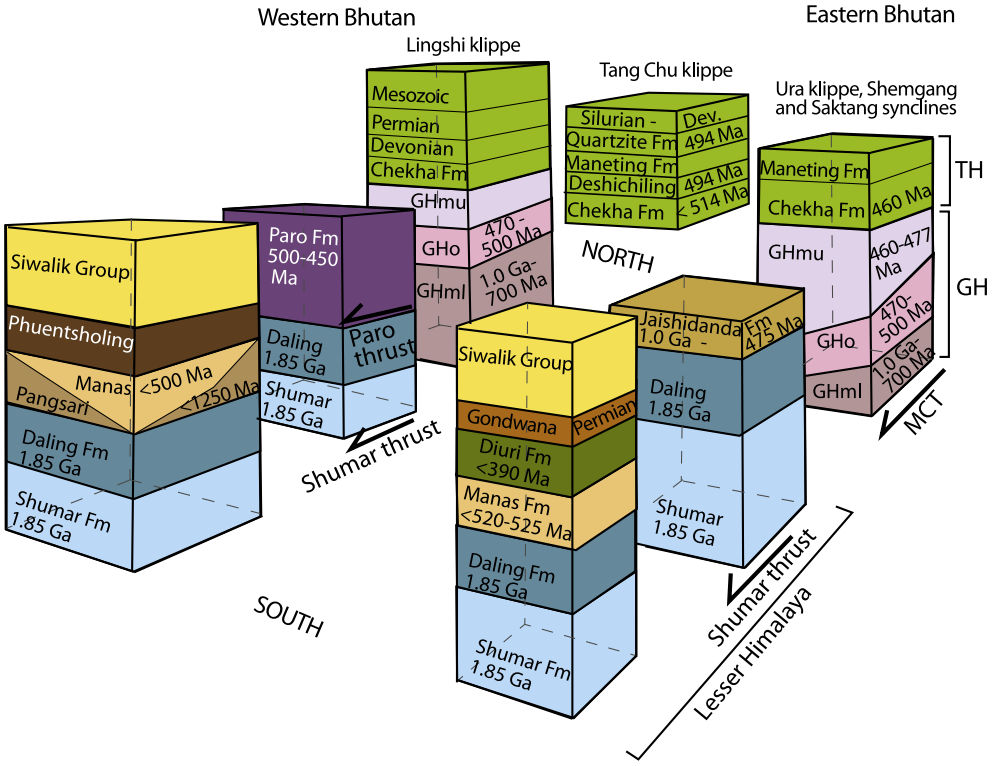

Fig. 2. Perspective stratigraphic columns for eastern and western Bhutan that illustrate north–south and east–west changes in formations and relative thickness changes. Estimates for stratigraphic thicknesses are provided in Table 2. GH, Greater Himalaya; LH lesser Himalaya; and GHml, GHo, and GHmu refer to Greater Himalayan lower metasedimentary unit, Greater Himalayan orthogneiss, and Greater Himalayan upper metasedimentary unit respectfully.

of ages, but a very low zircon yield (26 grains). It not only shows a large peak at 1.88 Ga, but also has a series of single grain ages at 1.2 Ga, 800, 685, 640, and 500 Ma (Fig. 5). Samples BU08-69B, BU10-90 and BU10-93 were collected from the Jainti Formation in south-central Bhutan (Fig. 3B). The youngest peak for sample BU08-69B is 991 Ma, with multiple peaks between ~950 Ma and 1.9 Ga. BU10-90 shows a DZ spectrum almost identical to BU10-89, with a youngest peak at 1.8 Ga. BU10-93 also had a very low zircon yield with 27 grains. However, 8 of these grains are young and cluster around 500 Ma. The next significant clustering of grains is at 1.8 and 1.9 Ga. BU07-60 is from the Phuentsholing Formation, and yielded one pronounced peak at 1.8 Ga. DZ spectra from samples BU07-61, BU10-71 and BU10-73 from the Pangsari Formation are quite similar, with the youngest peak at 1.7 Ga, and a range of peaks between 1.8 and 2.6 Ga (Fig. 5).

5.2. Epsilon Neodymium isotope geochemistry

Five shale and phyllite samples were analyzed for Sm and Nd isotopic ratios. Phuentsholing Formation samples BU08-139, BU10-66 and BU10-69 yielded εNd (0) values ranging between −24 and −26. Pangsari Formation samples BU08-136 and BU08-138 both yielded εNd (0) values of −27 (Table 2).

5.3. Carbonate C and O isotope measurements

Single samples from limestone and dolostone intervals in the Phuentsholing Formation (samples SBU 1, SBU 2, and SBU 4) yielded $\delta^{13}C$ values of −1.1‰, +1.2‰ and +1.6‰ respectively. Phuentsholing samples BU10-67, from a ~15 m dolomite bed, yielded $\delta^{13}C$ values ranging from +0.7‰ to +1.8‰, with most values between +1.6‰ and +1.8‰ (Fig. 6). Pangsari Formation sample SBU 3 contains 14 samples, which range from −0.5‰ to +1.3‰ with most values between +0.8‰ and +1.3‰. Pangsari Formation sample BU10-70 contains 16 samples, which yielded $\delta^{13}C$ values that range from −2.8‰ to +0.2‰. Jaishidanda Formation sample BU10-15 yielded the most positive $\delta^{13}C$ values, which range from +2.4‰ to +6.5‰. Paro Formation sample SBU 5 yielded $\delta^{13}C$ values that range from −1.2‰ to −1.6‰,

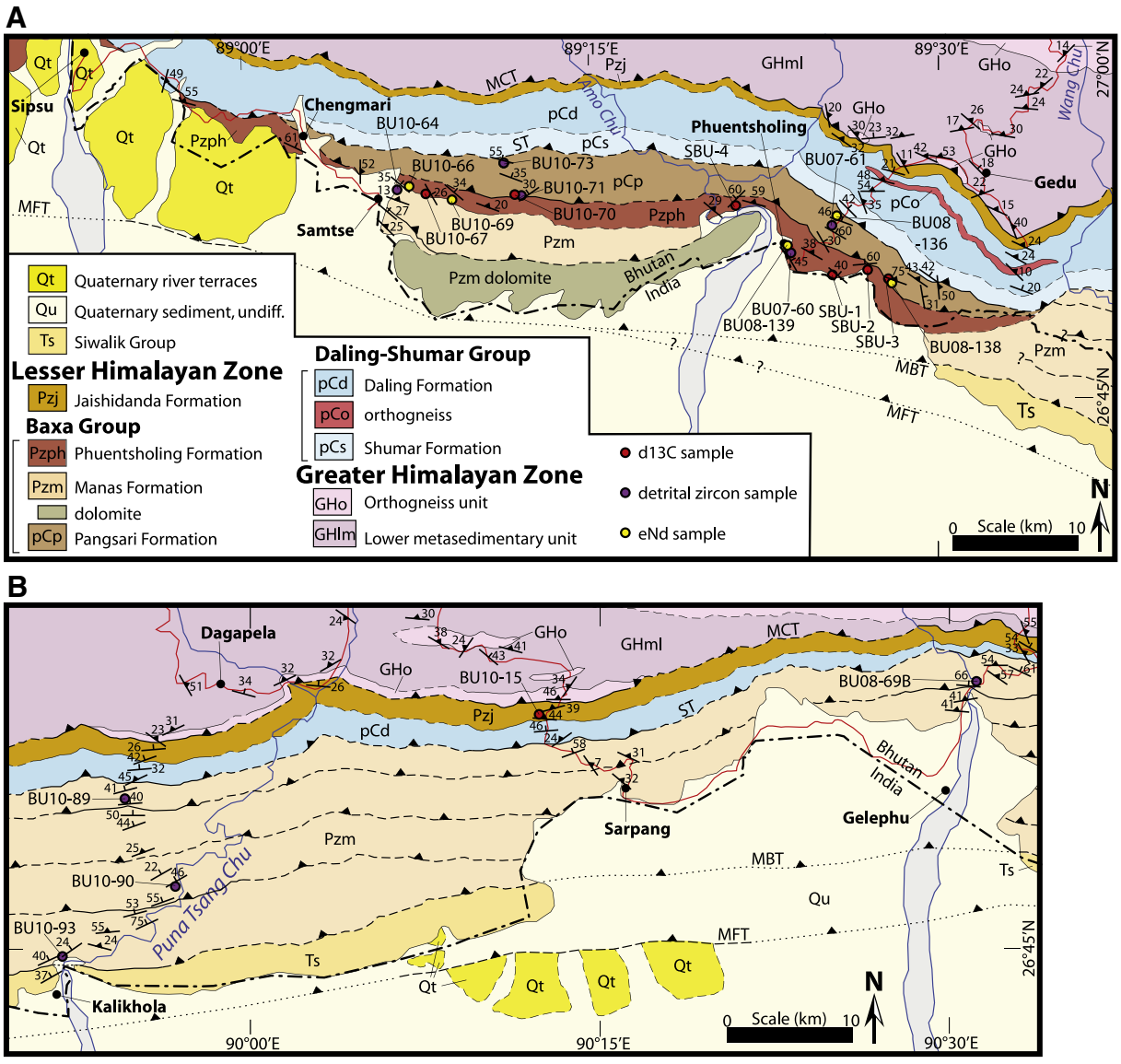

Fig. 3. Geologic maps of parts of southwest (A) and south-central (B) Bhutan. See Fig. 1 caption for structure abbreviations. The locations of all geochemistry samples are shown, and are color-coded based on the type of analysis.
Modified from Long et al. (2011c).

Table 2
Bhutan sample locations and lithologies.

Sample #	°E (dd.dddd)	°N (dd.dddd)	Formation	Lithology	Analysis
Greater Himalaya					
BU10-3	90.50602778	27.02125	GH upper seds	Quartzite	DZ
BU10-8	90.43594444	27.10261111	GH upper seds	Quartzite	DZ
BU10-20	90.22458333	26.93788889	GH lower seds	Quartzite	DZ
BU10-26	90.07552778	27.02730556	GH lower seds	Schist	DZ
BU10-30	90.07413889	27.09688889	GH upper seds	Quartzite	DZ
BU10-47	89.76808333	27.51480556	GH lower seds	Quartzite	DZ
BU10-50	89.24319444	27.23658333	GH lower seds	Quartzite	DZ
Chekha Formation					
BU07-56	91.63472222	27.35041667	Chekha	Quartzite	DZ
BU10-94	90.18	27.52930556	Chekha	Quartzite	DZ
Lesser Himalaya					
BU08-69B	90.51731	26.94117	Manas (Jainti)	Quartzite	DZ
BU10-89	89.90786	26.85717	Manas	Quartzite	DZ
BU10-90	89.94411	26.79442	Manas (Jainti)	Quartzite	DZ
BU10-93	89.86333	26.74447	Manas (Jainti)	Quartzite	DZ
BUO7-60	89.39319	26.85456	Phuentsholing	Quartzite	DZ
BUO7-61	89.42275	26.87372	Pangsari	Quartzite	DZ
BU10-64	89.11122	26.89972	Manas	Quartzite	DZ
BU10-71	89.20083	26.89519	Pangsari	Quartzite	DZ
BU10-73	89.18700	26.91847	Pangsari	Quartzite	DZ
BU08-136	89.42642	26.88008	Pangsari	Phyllite	eNd
BU08-138	89.46247	26.83556	Pangsari	Phyllite	eNd
BU08-139	89.39025	26.85875	Phuentsholing	Phyllite	eNd
BU10-66	89.12011	26.90158	Phuentsholing	Phyllite	eNd
BU10-69	89.15053	26.89178	Phuentsholing	Phyllite	eNd
SBU-1	89.42339	26.83908	Phuentsholing	Limestone	d13
SBU-2	89.44814	26.84189	Phuentsholing	Limestone	d13
SBU-3	89.46247	26.83556	Pangsari	Marble	d13
SBU-4	89.35394	26.88819	Phuentsholing	Dolomite	d13
BU10-67	89.13167	26.89647	Phuentsholing	Dolomite	d13
BU10-70	89.20083	26.89519	Pangsari	Dolomite	d13
BU10-15	90.20378	26.91750	Jaishidanda	Marble	d13
SBU-5	89.51458	27.27827	Paro	Marble	d13

and Paro Formation sample SBU 6 yielded $\delta^{13}C$ values that range from −2.9‰ to +3.7‰ (Fig. 6).

6. Deposition age and provenance constraints

6.1. Tethyan Himalayan rocks

Because of a lack of fossils, the Chekha Formation has previously been assigned an inferred Precambrian age (e.g., Gansser, 1983; Bhargava, 1995; Tangri and Pande, 1995). However, DZ peaks for our two new Chekha Formation samples yield Cambrian–Ordovician youngest grain populations (488–514 Ma). These ages agree well with previous studies that present Ordovician (460 Ma; Long and McQuarrie, 2010) and latest Cambrian (495–500 Ma; Hughes et al., 2010) youngest DZ peaks for TH strata from Bhutan (Fig. 4A). These data argue convincingly against a Neoproterozoic deposition age for the Chekha Formation.

Chekha Formation sample BU10-94 from the Tang Chu klippe has a youngest peak at 514 Ma. This peak is indistinguishable (within error) with the 494 and 500 Ma youngest peaks of the Deshichiling (WL-1) and Quartzite Formations (WL-270) that lie stratigraphically above it (Hughes et al., 2010). The Quartzite Formation contains age-diagnostic trilobite body fossils that are approximately 494 Myr old (Hughes et al., 2010). Thus, the simplest interpretation of the TH section preserved in the Tang Chu klippe is a relatively conformable stratigraphic succession, consisting of the Chekha, Deshichiling and Quartzite Formations, that are all latest Cambrian in age. Sample BU07-56 was collected near the base of the Chekha Formation in the Sakteng syncline in easternmost Bhutan. The youngest peak (488 Ma) is Ordovician in age, which provides further evidence that the base of the STD cuts through a thick Cambrian–Ordovician section at slightly different stratigraphic levels across-strike in Bhutan. In addition, in central Bhutan, Long and McQuarrie (2010) documented a 460 Ma youngest DZ peak in Chekha Formation quartzite, and argued that these rocks are in the footwall of the STDS. Previously published TH samples BU07-01 (Chekha Formation sample from the Ura klippe) and BU08-92 (Maneting Formation from Shemgang region) yielded ~900 Ma youngest peaks (McQuarrie et al., 2008; Long and McQuarrie, 2010). We suggest that this observed variability in DZ spectra in the Chekha Formation is the result of variation in sediment provenance.

Besides the pronounced late Cambrian–Ordovician peak, TH samples also exhibit several DZ peaks between 600 and 1200 Ma, and small peaks around 1.6–1.7 Ga. There are two possibilities for the source of these small 1.6–1.7 Ga peaks, northern Australia (Cawood and Korsch, 2008), and gneisses exposed in the Shillong Plateau and along the Brahmaputra River in Bangladesh (Ameen et al., 2007; Chatterjee et al., 2007; Yin et al., 2010a). Since 1.6–1.7 Ga peaks are common in DZ samples from Bhutan (Fig. 7) but less so in Himalayan samples in general (e.g., Gehrels et al., 2011) we suggest that the local source in the Shillong Plateau region is the most likely. However, this requires input into the system from the Indian shield. Late Neoproterozoic through 1.2 Ga peaks are common in many GH and TH samples across the Himalaya (DeCelles et al., 2000; Martin et al., 2005; Cawood et al., 2007; Myrow et al., 2010; Gehrels

Table 3
εNd isotopic analyses.

Sample	Formation	Sm	Nd	Sm/Nd	147Sm/144Nd
BU08-136	Pangsari	12.195	70.396	0.173235	0.104698
Bu08-138	Pangsari	6.507	38.448	0.169249	0.10229
BU08-139	Phuntsholing	6.5123	36.2	0.1799	0.10873
BU10-69	Phuntsholing	8.533	50.772	0.168058	0.101572
BU10-66	Phuntsholing	8.362	46.979	0.17799	0.107575

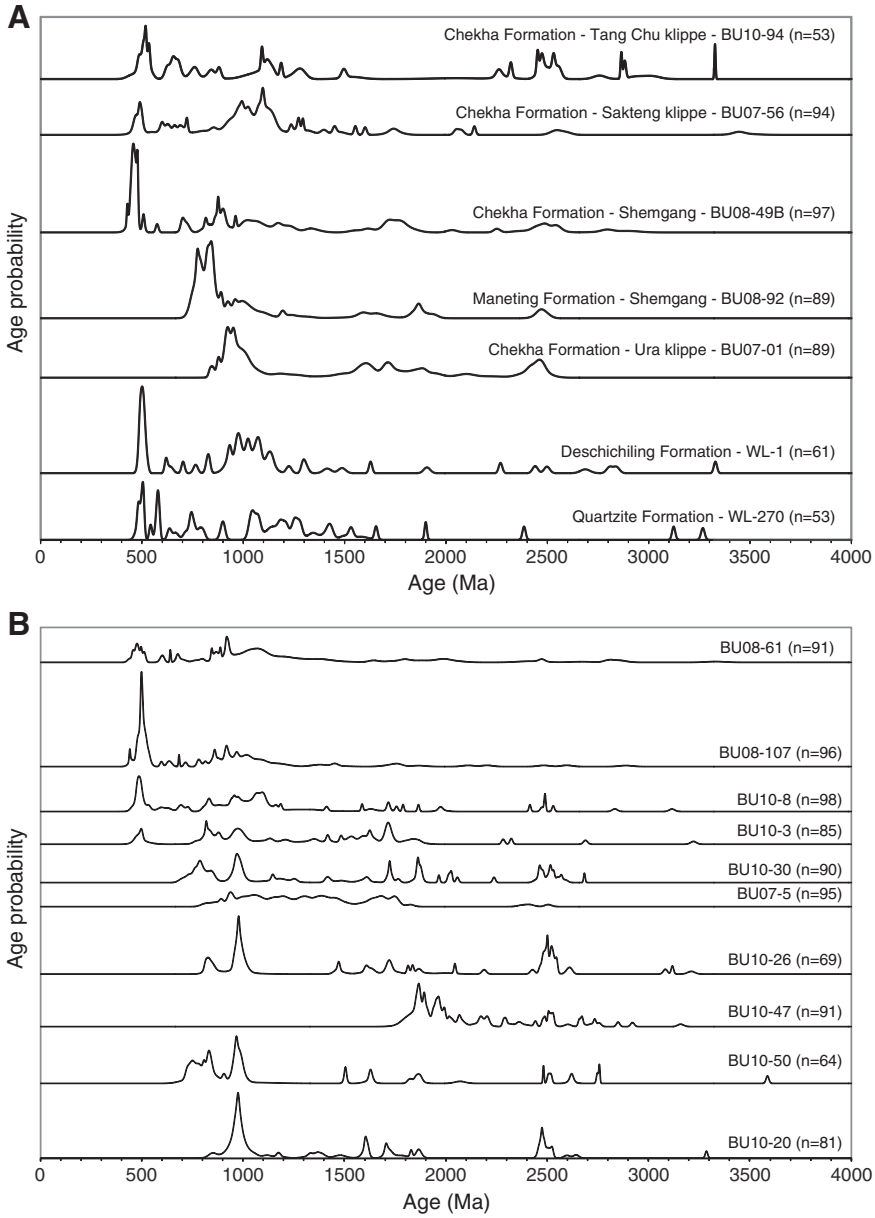

Fig. 4. U–Pb detrital zircon age spectra of Bhutan TH units (A) and GH units (B). Graphs are relative probability plots, which represent the sum of probability distributions from ages and corresponding errors (input errors are 1σ; same as shown in Table A1) for all analyses from each sample. See Fig. 3 for sample locations; see Table A1 for data from individual analyses, and Fig. A1 for Pb/U concordia plots of individual samples.

et al., 2011). The assembly of the Gondwana supercontinent in Late Neoproterozoic time created continent-scale orogens that produced voluminous detritus that was eventually deposited along the northern Indian margin (e.g., Cawood et al., 2007; Myrow et al., 2010). Although orogenic events such as the east African orogeny (680–500 Ma) and the Kuunga orogeny (570–530 Ma), which involved the collision of Australia and Antarctica with southern and eastern India, are probable sources for grains as young as 500 Ma (Meert, 2003; Cawood, 2005; Collins and Pisarevsky, 2005), we suggest that the significant late Cambrian–Ordovician peak observed in TH rocks in Bhutan had a more proximal source. Proximal, potential sources for this young (between 450 and 500 Ma) population of DZs are the widespread late Cambrian–Ordovician intrusions within the GH section, and coeval deformation and exhumation during the Cambrian–Ordovician orogenic event that affected the northern Indian margin (Hayden, 1904; Gehrels et al., 2006a; Cawood et al., 2007; McQuarrie et al., 2008). Although the young Cambrian–Ordovician zircon component is present in most of our TH samples, the lack of similar-aged zircons in the Maneting Formation (which overlies the Chekha Formation in the Shemgang region) and in the Chekha Formation exposed in the Ura Klippe, suggests that the source for the Cambrian–Ordovician zircons was not ubiquitous during the depositional history. In addition, the Maneting Formation overlies Ordovician-aged Chekha Formation in the Shemgang region (Long and McQuarrie, 2010), but underlies the late Cambrian Quartzite Formation in the Tang Chu klippe (Hughes et al., 2010). This suggests that the late Cambrian–Ordovician depositional system, although dominated by coarse-grained detritus, had important fine-grained components that varied in both space and time through the basin, and that the current formation names based on fine-grained (Maneting) or coarse-grained components (Chekha, Quartzite Formation) are misleading. However, what our study emphasizes is that the mapped Chekha, Maneting and Quartzite Formations were all deposited in latest Cambrian to early Ordovician time throughout Bhutan.

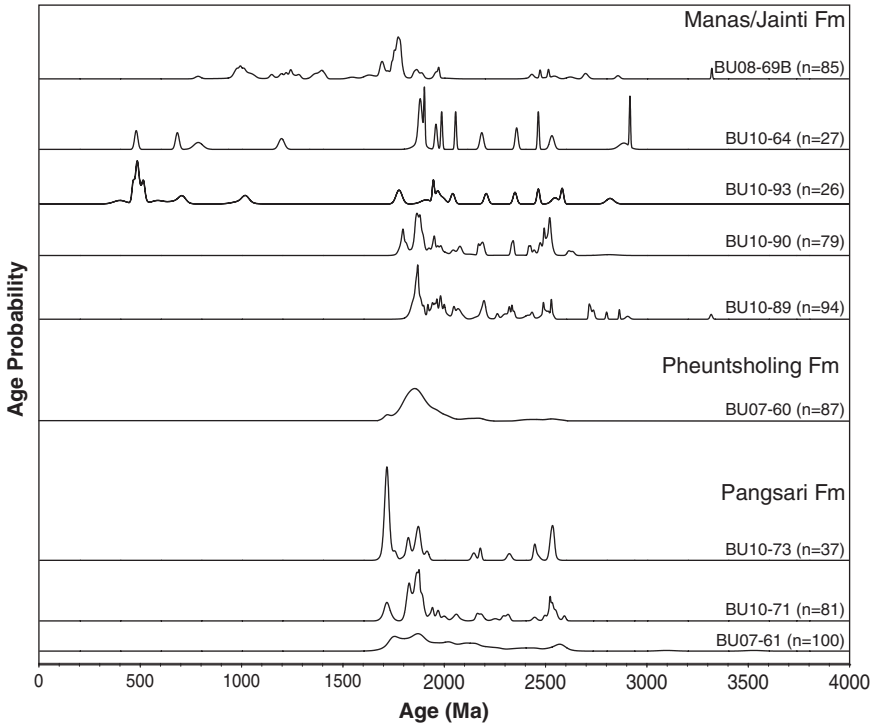

Fig. 5. U–Pb detrital zircon age spectra of Bhutan LH units. Graphs are relative probability plots, which represent the sum of probability distributions from ages and corresponding errors (input errors are 1σ; same as shown in Table A1) for all analyses from each sample. See Table 2 and Fig. 3 for sample locations; see Table A1 for data from individual analyses, and Fig. A1 for Pb/U concordia plots of individual samples.

6.2. Greater Himalayan rocks

Samples analyzed from the lower metasedimentary unit of the GH section all contained Neoproterozoic or older DZs. BU10-26, BU10-50, and BU10-20 contained the youngest detrital peaks between 724 and 974 Ma. Combining these samples with those previously published (Long and McQuarrie, 2010) shows a general younging trend of youngest DZ peaks moving upsection from the MCT (Fig. 4B). The notable outlier to this is sample BU10-47 which displays a Paleoproterozoic youngest peak at 1.8 Ga. The lower metasedimentary unit of the GH section is intruded by late Cambrian–Ordovician age (480–500 Ma) plutons (Long and McQuarrie, 2010) so at the top of the section, the age of the sedimentary protolith must be younger than 724 Ma and older than ~500 Ma. The younging-upward trend in youngest DZ peaks continues into the upper metasedimentary unit of the GH section. Combining the new data presented here with previously published ages (Long and McQuarrie, 2010) demonstrates that almost all of the youngest DZ peaks in the upper metasedimentary unit are late Cambrian–Ordovician (between 460 and 477 Ma). BU10-30 is the only sample from the upper metasedimentary unit that lacks the young Ordovician grains. We suggest that the depositional age of the GH upper metasedimentary unit is identical to the age of the youngest detrital zircons (~477–460 Ma), and similar to our interpretations for the Chekha Formation, that the observed variability in DZ spectra may be the result of provenance from a heterogeneous source region with an aerially-limited source for Paleozoic zircons.

Like the TH samples, GH DZs also have significant peaks between 600 and 1200 Ma, and around 1.6–1.7 Ga. In the GH lower metasedimentary unit, the likely source of these grains is the orogenic belts associated with the assembly of Gondwana in Late Neoproterozoic time (e.g., Myrow et al., 2010; Gehrels et al., 2011). The Paleoproterozoic youngest peak of BU10-47 highlights that although not common, there still were periods of time between 900 and 600 Ma when the sediment source may have been exclusively from the Indian Shield. We suggest that during deposition of the upper metasedimentary unit, the sediment source for these rocks was the same as we interpret for overlying TH strata, which is from uplift and exhumation of a deforming lower metasedimentary GH section that contains late Cambrian–Ordovician intrusions (e.g., Gehrels et al., 2003, 2011). The young, 477–460 Ma DZs that define the GH upper metasedimentary unit are identical to the DZ spectra of the TH samples that are stratigraphically and structurally above them. Derivation from the lower GH section is also suggested by the increase in abundance of 1.0–1.2 Ga ages, and the shift to slightly younger Cambro-Ordovician age peaks upsection (Gehrels et al., 2011).

6.3. Lesser Himalayan rocks

6.3.1. Baxa Group

The type section of the Baxa Group (Sengupta and Raina, 1978; Gansser, 1983; Tangri, 1995; Long et al., 2011a) was originally defined in the Duars (foothills) of southwest Bhutan (Mallett, 1875; Acharyya, 1974) (Fig. 3A, eastern edge). Bhargava (1995) divided the Baxa Group into four formations, the Manas, Jainti, Phuentsholing and Pangsari Formations based on varying lithology and/or color. However, there is no location where all four formations of the Baxa Group are present, making the original depositional relationships of these formations uncertain. Martin et al. (2011) noted that the Baxa Group in Sikkim and western Bhutan is lithologically very similar to the Mesoproterozoic(?) Syangja-Malekhu succession in central Nepal, specifically with the presence of variegated green, pink, and yellowish-white calcareous slate and bluish-gray stromatolitic dolostone (Bhattacharyya and Mitra, 2009), and suggested that the Baxa Group in western Bhutan could represent a dramatically different age, provenance and depositional environment than the Manas Formation of the Baxa Group in eastern Bhutan and correlative strata (Menga Limestone, Chillipam Dolostone, and Rupa/Dedza Dolostone) in Arunachal Pradesh (Yin et al., 2010b).

The Manas Formation exhibits youngest DZ peaks that range in age from 1.8 Ga to 500 Ma. The youngest age population was identified in two samples (BU10-93 and BU10-64), both of which had low zircon yields (27 and 26 grains respectively) but contained young grains. The

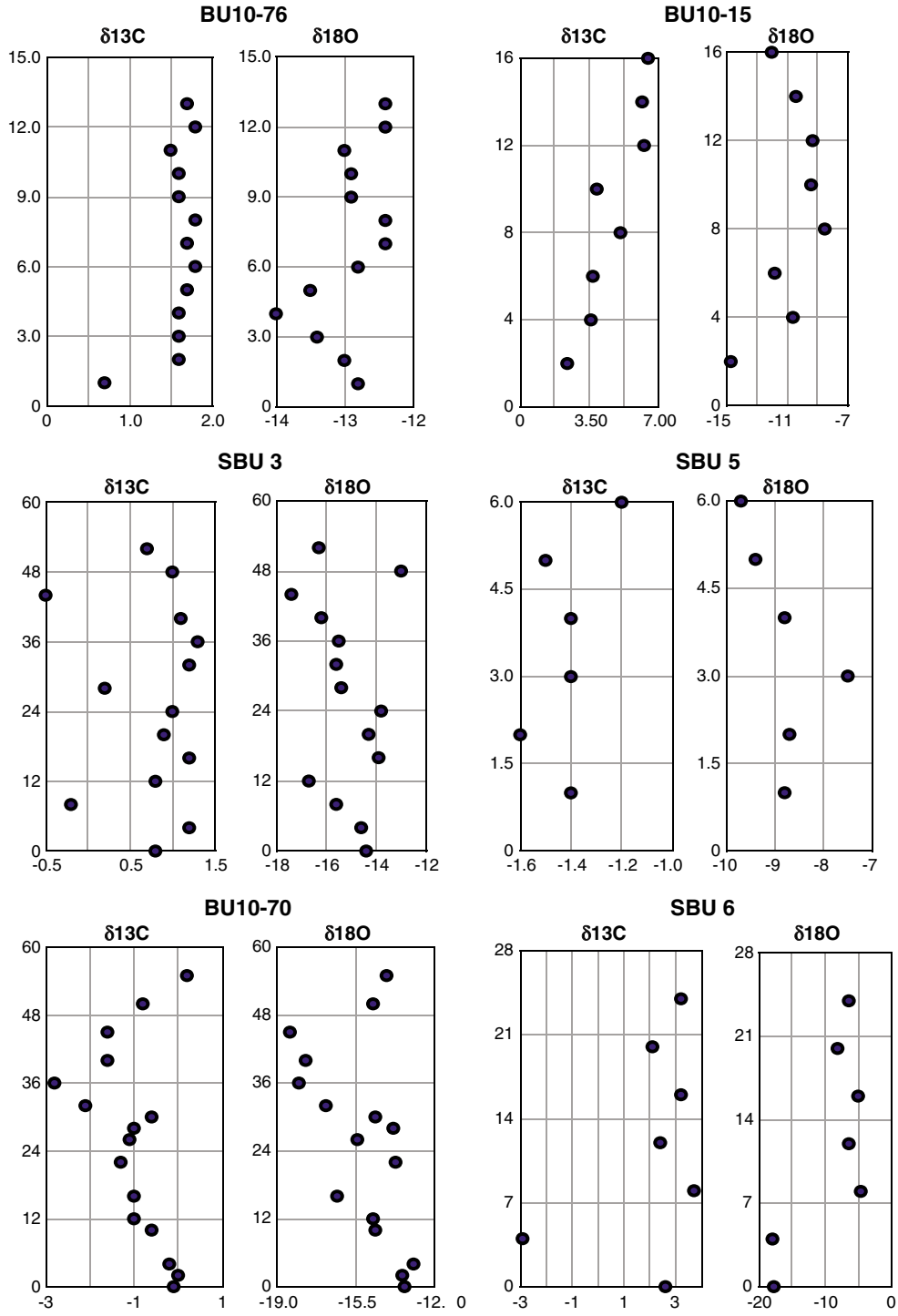

Fig. 6. $\delta^{13}C$ and $\delta 18O$ data versus stratigraphic position for Bhutan LH section and Paro Formation. Data for individual analyses are shown in Table A3.

four youngest grains of sample BU10-64 fail to define a peak of three or more grains, although the presence of these four concordant grains (Appendix 1) suggests that this sample is Neoproterozoic or younger in age. The young peak of sample BU10-93 is more robust with eight grains that cluster around 500 Ma. Both BU10-93 and BU10-64 were collected from Baxa Group thrust sheets that restore proximal to India.

Phuentsholing and Pangsari Formation samples have Paleoproterozoic youngest DZ peaks. The single Phuentsholing Formation sample yields a broad peak centered at 1.8 Ga whereas the three Pangsari Formation samples each display youngest peaks at 1.7 Ga (Fig. 5). εNd values from the Phuentsholing and Pangsari Formations also confirm that the detritus entering the basin was old. Because of the pronounced swings in $\delta^{13}C$ values during the late Neoproterozoic (Fig. 8), we analyzed the $\delta^{13}C$ and $\delta^{18}O$ values of Phuentsholing and Pangsari Formation carbonates to see if we would detect any of the variations typical of this time period (e.g., Halverson et al., 2005; Maloof et al., 2005; Kaufman et al., 2006, 2007). Neither formation showed the strong excursions that typify the late Neoproterozoic. Values for these formations ranged from −2.8‰ to +1.8‰. During the late Paleoproterozoic through ~1250 Ma, marine carbonate shows very little variability in $\delta^{13}C$ values. Most values lie within 1‰ of zero with a few excursions to −2‰ (Fig. 8). Post-1250 Ma $\delta^{13}C$ values vary between −2.0‰ and +3.8‰ until the mid-

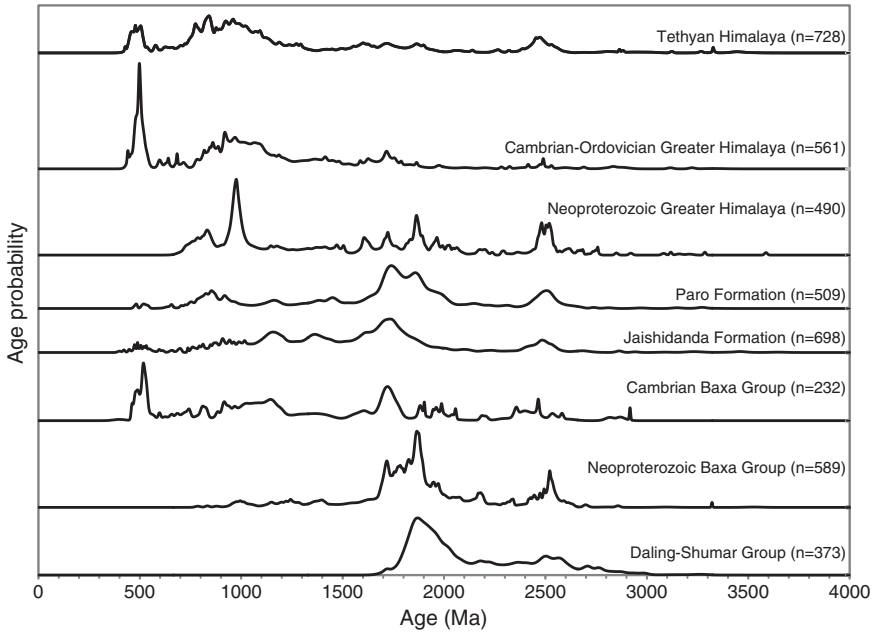

Fig. 7. Cumulative U–Pb detrital zircon age spectra for LH, TH, and GH units in Bhutan LH. Graphs are relative probability plots, which represent the sum of probability distributions from ages and corresponding errors (input errors are 1σ; same as shown in Table A1) for all analyses from each sample.

to late-Neoproterozoic where excursions greater than ±5‰ are common. Thus the depositional ages of the Phuentsholing and Pangsari Formations are likely to be younger than 1250 Ma. In the field, we did not recognize a fault between the site where we collected the Manas Formation sample BU10-64, which contains four grains between 500 and 700 Ma and the site where we collected Phuentsholing Formation sample BU10-67, which has $\delta^{13}C$ values that range from +0.7‰ to +1.8‰ with most values between +1.6‰ and +1.8‰ (Figs. 3, 6). Field relationships suggest that the medium to thick-bedded quartzite that comprises the Manas Formation is gradually stratigraphically replaced by progressively-thicker beds of phyllite and dark gray to black slate, until the unit contains only a few thin beds of dark-brown, fine-medium grained quartzite. In other words, based on field relationships, we interpret that the Manas Formation fines upwards into the Phuentsholing Formation. Thus if the Manas Formation is ~500 Ma in age (Long et al., 2011a; this study), we would suggest that the Phuentsholing Formation is younger, and was deposited during minor ±2–3‰ $\delta^{13}C$ excursions that were present between ~523 and ~500 Ma (Maloof et al., 2005; 2010). The Pangsari Formation is in all cases in fault contact with the rest of the Baxa Group (Long et al., 2011d) (Fig. 3), thus we can only recommend that the Pangsari Formation is younger than ~1250 Ma.

All Baxa Group samples in western Bhutan consistently show significant Paleoproterozoic (~1.7–1.8 Ga) DZ peaks (Fig. 5). Central Bhutan sample BU08-69B also contains a significant component of 900–1700 Ma grains that are essentially absent from Phuentsholing and Pangsari Formation samples. BU08-69B closely matches DZ spectra from Manas Formation samples in eastern Bhutan (Long et al., 2011a), but lacks the young peaks (i.e. Cambrian Baxa Group, Fig. 7). Based on the presence of young grains in samples BU10-93 and BU10-64, and the map relationship between the Manas Formation and the Phuentsholing Formation, we propose that their deposition age is ~500 Ma. The lack of DZs in the range of 1300–500 Ma in the Phuentsholing Formation (BU07-60) and Baxa Group samples BU10-90 and BU10-89 and the very limited number from the Manas Formation from western Bhutan suggest that the Baxa Group in western Bhutan was sourced almost exclusively from the Indian Shield. The samples that contain the youngest grains, BU10-93 and BU10-64, are from Baxa Group samples that restore the closest to India. This suggests that the source of the Cambrian to Neoproterozoic age grains was from the south, such as the Kuunga orogen to the southeast or possibly the East African Orogen to the southwest (Cawood, 2005; Cawood and Buchan, 2007; Myrow et al., 2010).

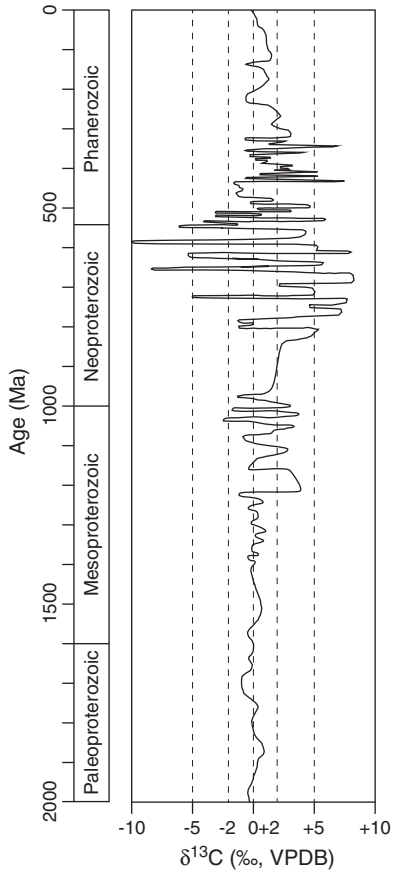

Fig. 8. Cumulative $\delta^{13}C$ and $\delta^{18}O$ curve illustrating values of marine carbonate during the Proterozoic and Phanerozoic.
Modified from Martin et al. (2011) and Bartley and Kah, (2001), using data from Kah et al. (1999), Bartley et al. (2001), Halverson et al. (2005), Saltzman (2005), and Maloof et al. (2005).

That Neoproterozoic grains are present in all of the Baxa Group samples from eastern Bhutan and strong Cambrian peaks are present in half of the samples (Long et al., 2011a) suggests that the source for these grains was from the southeast.

6.3.2. Jaishidanda Formation

DZs from the Jaishidanda Formation have been described in Long et al. (2011a) and Tobgay et al. (2010). Of the eight samples analyzed, three samples contain Cambrian–Ordovician age zircons with ages that

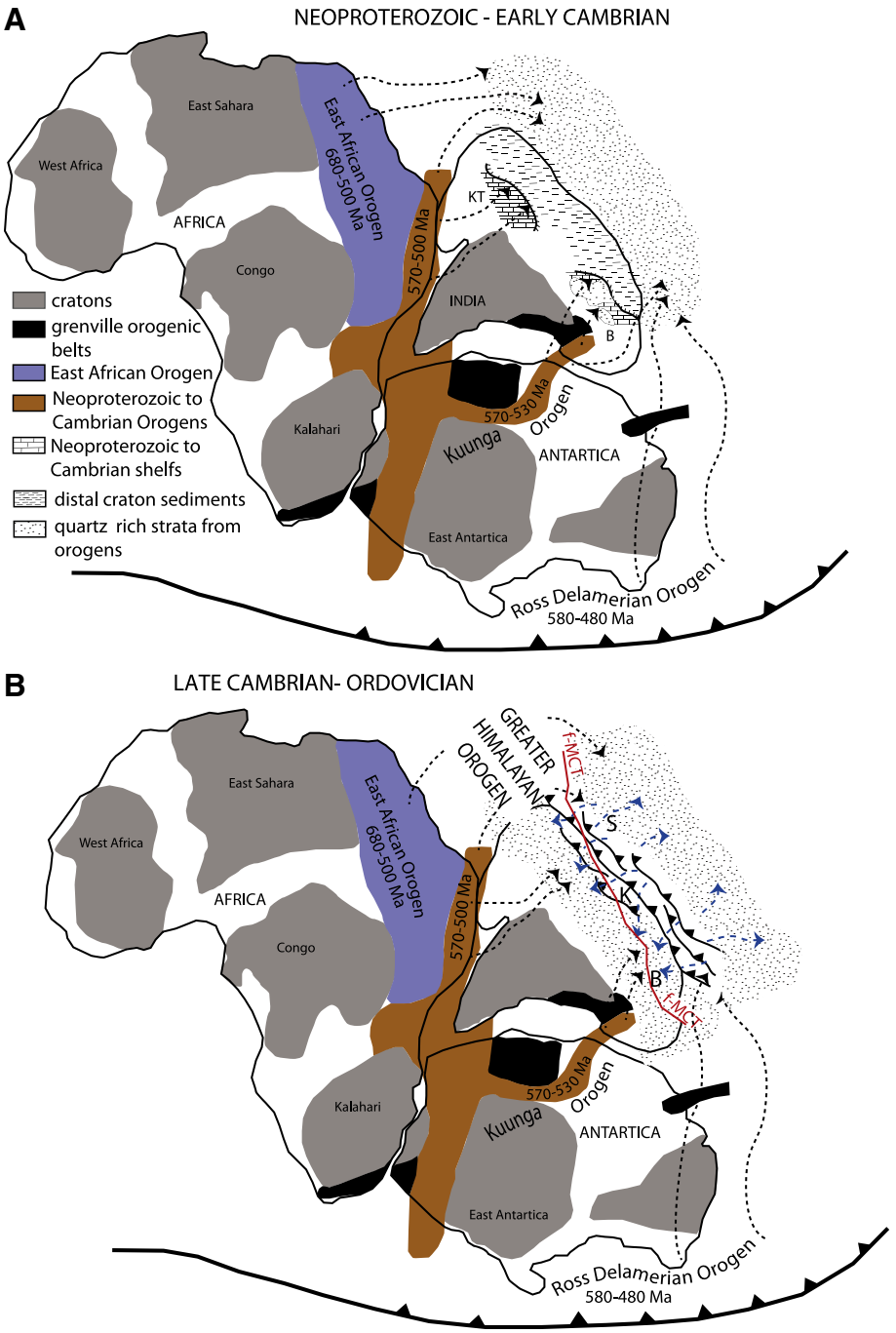

Fig. 9. Reconstruction of Gondwana supercontinent in the late Neoproterozoic (A) and the Cambro-Ordovician (B). Sediment transport paths are diagrammatic to illustrate probable sources. Panel A highlights potential drainage systems that may have been sourced from the early Cambrian orogens on the eastern and western edges of India. We argue that the location of the Neoproteozoic–early Cambrian platform deposits in the eastern and western Himalaya are linked to drainage systems that were limited to the eastern and western edges of the Indian continent. Uniformity in the DZ spectra of the outboard GH and TH strata is due to mixing via large margin-parallel transport systems. The Paro and Jaishidanda Formations would restore medially between these two systems. Panel B highlights our hypothesis of how the transport systems changed in the Cambro-Ordovician when the depositional environment switched from open ocean conditions to an active margin. We suggest that the dramatic increase in sedimentation thickness, clast size and input of Ordovician detritus observed in the GH and TH sections require a more proximal source, such as the uplifted Greater Himalayan rocks and Cambrian–Ordovician granites intruding the Greater Himalayan sequence. B, Bhutan section; KT, Krol-Tal section; K, Kathmandu section; S, Spiti section; red line and F-MCT mark the future location of the Main Central Thrust; see text for discussion.
Modified from Myrow et al. (2010).

range from 475 to 549 Ma. All samples yield peaks between 0.9 and 1.7 Ma. Long et al. (2011a) presented two options for the difference in youngest age zircons. First, the entire unit is Ordovician or younger, and the observed variability in DZ spectra is the result of variation in sediment provenance. Thus, a small areal extent and/or transport distances or paths would have limited the source for these young zircons. Alternatively, although the lithology of the Jaishidanda Formation is uniform along strike, the unit could contain strata that range from Neoproterozoic through Ordovician. The $\delta^{13}C$ data we present in this study help address this uncertainty. $\delta^{13}C$ values from a ~16 m-thick marble bed within the Jaishidanda Formation range from +2.4‰ to +6.5‰ (Fig. 6). The most likely window of time for positive excursions of this magnitude is in late Neoproterozoic to early Cambrian time (Fig. 8), although there is also a brief excursion up to +7‰ in the late Ordovician (Saltzman, 2005). The +6.5‰ $\delta^{13}C$ data values are quite similar to those obtained from Baxa Group (Manas Formation) dolomite in eastern Bhutan, on samples that were bracketed between 525 and 520 Ma (Long et al., 2011a). We suggest that the positive excursion recorded in the Jaishidanda Formation marble argues for a wider depositional time window for the formation (late Neoproterozoic through Ordovician).

The 1.7 Ga peak observed in most Jaishidanda Formation samples has a likely source just south of Bhutan (Ameen et al., 2007; Chatterjee et al., 2007; Yin et al., 2010a; Long et al., 2011a). We suggest that the source for young Ordovician DZs was exhumation of GH sedimentary protoliths and granite intrusions, which were undergoing deformation at this time (e.g., Gehrels et al., 2003; Cawood et al., 2007). An environment that would match both of these constraints is a retro-arc foreland basin caught between the deforming northern margin of the Indian continent (e.g., Cawood et al., 2007) and the stable craton to the south. The Jaishidanda Formation would represent the distal, southern most limit of the foreland basin proposed by Gehrels et al. (2003, 2006a, 2006b), while still receiving a component of sediment from the Indian craton. A Neoproterozoic through Ordovician age for upper LH strata makes them time-equivalent with TH strata (e.g., Myrow et al., 2003, 2010; McQuarrie et al., 2008; Gehrels et al., 2011). We hypothesize that rocks in both of these tectonostratigraphic zones represent overlap strata deposited during or shortly after proposed Cambrian–Ordovician deformation along the northern Indian margin.

6.3.3. Paro Formation

DZ spectra within the Paro Formation are highly variable, with peaks at ~0.5, 0.8, 1.2, 1.4, 1.7, 1.8, and 2.5 Ga (Tobgay et al., 2010). In addition, εNd values sampled from schist or phyllite had more positive values that range from −12 to −16, similar to the −12.9 εNd (0) value of a 450 Ma granite intrusion within the Paro Formation. Tobgay et al. (2010) used the youngest DZ peaks, the less negative εNd values, which require younger detritus, and the presence of ~450 Ma orthogneiss bodies that intrude the formation in several locations to argue for a Cambro-Ordovician deposition age range. The two Paro Formation marble bands that we analyzed for $\delta^{13}C$ and $\delta^{18}O$ yield values ranging from −2.9‰ to +3.7‰ (Fig. 6), which is compatible with values recorded in the Late Cambrian and Late Ordovician (Fig. 8) (Saltzman, 2005; Maloof et al., 2005; 2010).

The combination of samples with only Paleoproterozoic DZs in depositional contact with samples that contain Cambrian DZs and less negative εNd values, requires both old and young sources of detritus. Two samples from the Paro Formation contain exclusively Paleoproterozoic (~1.8 Ga) DZs, requiring one of the principle sediment sources to be from the Indian shield. The ~500 Ma DZs require a Cambrian source, either from the north (GH rocks or granite intrusions) or from the southeast (Kuunga orogen). Many of the other peaks between 0.8, 1.2, 1.4, and 1.7 Ga are common in both GH and LH samples from the region. There is no coherent pattern in the age distribution of DZs moving stratigraphically up through the Paro Formation, and the first-order variation in εNd (0) values is between shale and sandstone protoliths (Tobgay et al., 2010). Tobgay et al. (2010) suggested that the Paro Formation accumulated in a depositional setting characterized by abrupt changes in detrital input. This could have resulted from a combination of active tectonics or a heterogeneous source region, as well as limited mixing of sediment within the basin (e.g., DeGraaff-Surpless et al., 2003). We suggest that the Paro Formation was deposited in a basin similar to the one previously described for the Jaishidanda Formation

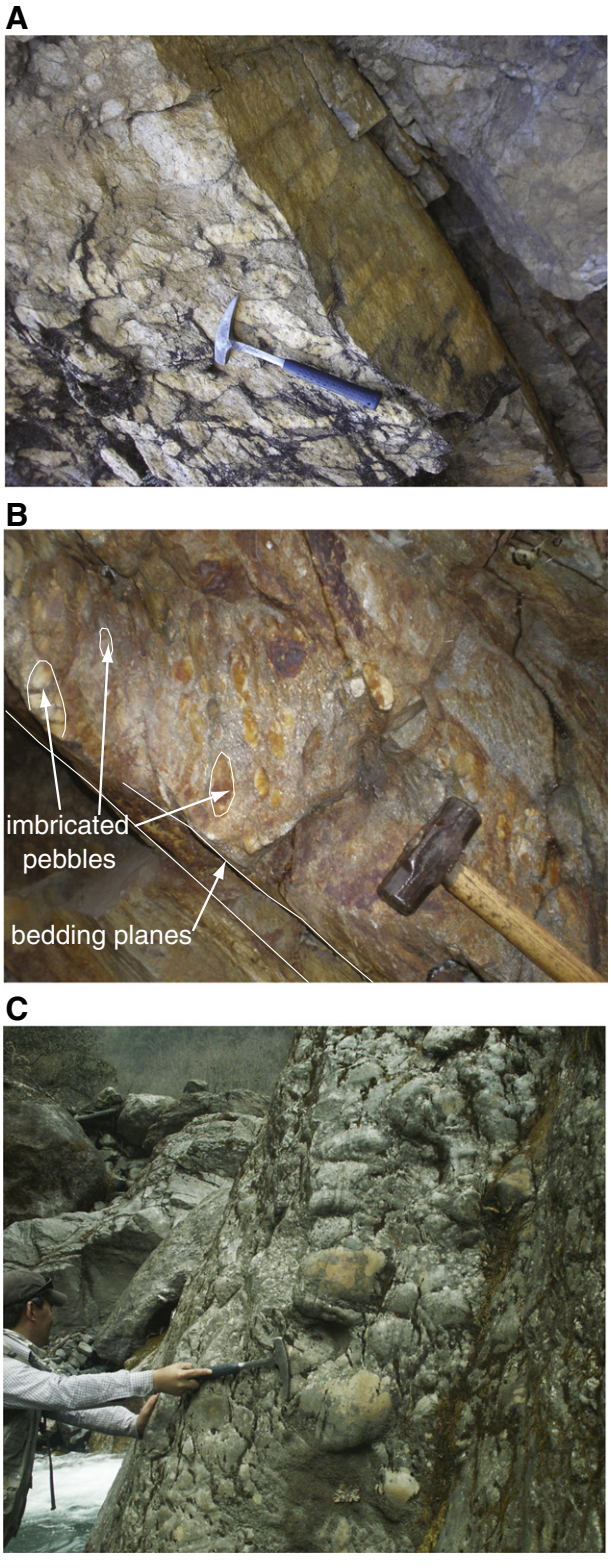

Fig. 10. Photos of Ordovician conglomerates in Bhutan: A, Paro section. B, Shemgang section central Bhutan, Beds dip to the north. C, Sakteng section.

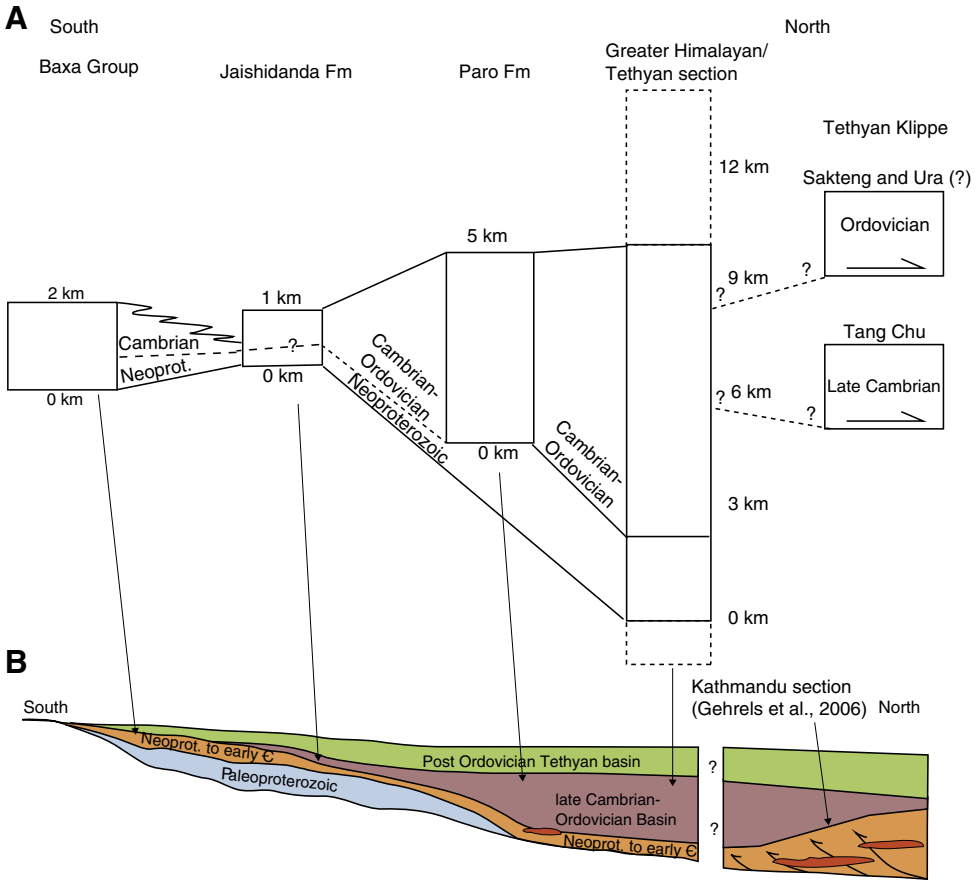

Fig. 11. Diagram highlighting spatial variations, thickness variations and age constraints for the Cambro-Ordovician basin in Bhutan (A), and cartoon illustrating the proposed geometry of the northern Indian margin at ~450 Ma (B). Dashed box in B (GH column) shows estimated thickness by removing 50% flattening strain; see text for details.

and represents a region more proximal to the GH rocks undergoing deformation. The similarity in the DZ spectra of the Paro and Jaishidanda Formations (Fig. 7) suggests that both units shared this relative, medial basin position (Tobgay et al., 2010).

7. Discussion

7.1. Variations and similarities in sediment source/provenance

The TH, Cambrian–Ordovician GH, Paro Formation, Jaishidanda Formation and Cambrian Baxa Group show marked similarities in DZ spectra (Fig. 7). Similarity in DZ spectra of Cambrian through Ordovician strata along the east to west extent of the Himalayan arc was documented by Myrow et al. (2010). The study by Gehrels et al. (2011) showed that TH and correlative Cambrian and younger LH DZ spectra also displayed clear similarities in strata extending from Cambrian through Cretaceous in age. The DZ age populations that dominate in both of these studies are 480–570 Ma, 750–1200 Ma, and 2430–2560 Ma. Cambrian–Ordovician samples from Bhutan that are classified as LH (Paro Formation, Jaishidanda Formation and Baxa Group) exhibit these three dominant age groups, but also show a pronounced peak at 1.6–1.8 Ga, which we interpret as being derived from the proximal Indian shield (Ameen et al., 2007; Chatterjee et al., 2007; Yin et al., 2010a; Long et al., 2011a). The units that restore to a more northerly position (TH, Cambrian–Ordovician GH, Paro Formation, Jaishidanda Formation) all contain Ordovician grains, whereas the Cambrian Baxa Group has no grains younger than 500 Ma.

The Baxa Group shows significant changes in provenance from north to south, as well as from east to west. Baxa Group samples with young DZ components, including BU07-22 and NBH-18 from eastern Bhutan (McQuarrie et al., 2008; Long et al., 2011a) and BU10-93 and BU10-64 from western Bhutan are the southernmost samples collected. In the case of BU10-93 and BU10-64, these samples are from exposures within a few kilometers of the Indian foreland. Baxa Group samples farther to the north do not yield the young ages. In addition there is a pronounced change from east to west. Manas Formation samples from eastern Bhutan all contain peaks that range from 1.0 to 1.7 Ga (Long et al., 2011a). Central Bhutan sample BU08-69B from the Jainti Formation has an identical range in ages. Samples from western Bhutan that have young 500 Ma grains (BU10-93 and BU10-64) do not display the intermediate peaks from 1.0 to 1.7 Ga. Instead, the next dominant grain populations are at ~1.8 Ga. We suggest that the 500 Ma grains as well as the 1.0 to 1.7 Ma grains were sourced from the Grenville and late Neoproterozoic to Cambrian orogens along the eastern side of India (Cawood, 2005; Cawood and Buchan, 2007; Myrow et al., 2010). The loss of this signal to the north and west in the Baxa Group basin may indicate that the river systems that transported the detritus were confined to the eastern edge of the Indian continent and that deposition was limited to areas proximal to the river outlets. The northwestern-most Baxa Group samples only received sediment input from the Indian Shield (indicated by solely 1.7–1.9 Ga grains).

While there is significant similarity between LH, GH, and TH Neoproterozoic–Ordovician strata (Myrow et al., 2010; McKenzie et al., 2011), for samples that restore close to the Indian shield such as the Baxa Group samples from eastern Bhutan (Long et al., 2011a) or the Tal samples from the LH zone of northwest India (Myrow et al., 2003, 2010), the deposition and preservation of these strata may be a function of proximity to the large transport systems delivering detritus from cratonic India to the northern Indian margin, while the uniformity in the DZ spectra of the more distal GH and TH strata is due to mixing via large, margin-parallel transport systems (Fig. 9). Particularly for the Baxa Group, we suggest that the river systems that crossed the craton

were sourced from the Neoproterozoic through Cambrian orogenic belts that rim India (e.g., Myrow et al., 2010).

The late Cambrian–Ordovician GH and TH sections, the Paro Formation and the Jaishidanda Formation all contain a young, dominantly Ordovician DZ population. Proximal sources for this component are the late Cambrian–Ordovician intrusions within the GH section that are linked to coeval deformation and exhumation of the older (Neoproterozoic–Cambrian) GH rocks (Hayden, 1904; Gehrels et al., 2003, 2006a; Cawood et al., 2007). As suggested in Gehrels et al. (2011), additional support for derivation from the GH section is an increase in abundance of 1.0–1.2 Ga ages (which matches the higher proportions found in GH samples), and a shift to slightly younger Cambrian–Ordovician age peaks in the Ordovician strata (Fig. 4). The presence of coarse conglomerates of Ordovician age in TH rocks south of the GH (e.g., Gehrels et al., 2003, 2006a, 2006b; Long and McQuarrie, 2010) (Fig. 10) also argues for a proximal source, as opposed to derivation entirely from distant sources. Thus the late Cambrian–Ordovician time represents a switch from the open ocean environment that characterized the Neoproterozoic through early Cambrian of the region (e.g. Collins and Pisarevsky, 2005) to an active margin (Cawood et al., 2007; Gehrels et al., 2011). The Paro and Jaishidanda Formations would restore at a medial position between the Indian shield and the orogen preserved in GH rocks. We suggest that both formations received detritus from the north (the late Cambrian–Ordovician grains) and south (the older Proterozoic grains), and in the case of the Paro Formation the marked difference in εNd (0) values between shale and sandstone protoliths requires very limited mixing in the basin (Tobgay et al., 2010).

7.2. Timing relationships between LH, GH, and TH deposition

Fig. 11 shows spatial patterns, thickness variations and deposition age constraints for the Cambrian–Ordovician basin in Bhutan. The GH section preserved a Neoproterozoic through possibly lower Cambrian section at its base. In central Bhutan this is 3 km thick, whereas in western Bhutan it reaches a thickness of 6 km. Both the Jaishidanda Formation and the Baxa Group may preserve a Neoproterozoic section at their base. Currently there are no data that can constrain the thickness of this possible Neoproterozoic section or how that thickness may vary from east to west. The Pangsari Formation of the Baxa Group (~2 km thick) may represent an early Neoproterozoic part of the basin. Proximal shelf deposition continued through the lower Cambrian and is recorded in the quartzite-rich Manas Formation that typifies eastern Bhutan. The depositional environment and accommodation space dramatically changed in the late Cambrian. The minimum thickness of the late Cambrian–Ordovician basin was up to ~7 km thick in central Bhutan (combined GH and TH sections) (Long and McQuarrie, 2010), with a ~5.5 km-thick medial portion (Paro Formation), and thinning down to a preserved thickness of <1.5 km at its southern extent (the Jaishidanda Formation). These thicknesses do not account for internal strain documented in these rocks. Detailed strain studies through the GH–TH section in central Bhutan, which preserves the thickest section of late Cambrian–Ordovician quartzite, indicate ~100% flattening at the base of the section and 30% flattening towards the top (Long and McQuarrie, 2010; Long et al., 2011c; Corrie et al., 2012). An average through the entire section is 50%. Restoring the strain implies an original stratigraphic section possibly as thick as 14 km that was deposited between ~500–450 Ma, which would equate to sedimentation rates of 0.28 + mm/yr. Himalayan orogenesis has in places thickened the original GH stratigraphic section and these thrust faults are recognizable by an abrupt change in pressure and temperature (Grujic et al., 2002; Kohn, 2008). However, there are no abrupt changes in pressure or temperature conditions observed through the entire 10 km thick GH through TH section preserved in central Bhutan (Corrie et al., 2012).

Although the southern limit of the Jaishidanda Formation is not preserved at the surface, we hypothesize that the Ordovician Jaishidanda Formation onlapped onto the dominantly early Cambrian Baxa Group toward the south, and pinched out north of where the Baxa Group is exposed at the surface today (Long et al., 2011b). Both the Jaishidanda Formation and the Baxa Group were deposited on the 1.8 Ga Daling Formation and, in the southern part of Bhutan, the Permian Diuri Formation rests on the Baxa Group (Long et al., 2011a). Thus the pinch out of the Ordovician portion of the Jaishidanda Formation must be north of the exposed Baxa/Diuri contact. In Bhutan the northern limit of the late Cambrian–Ordovician basin is unknown. However in Nepal it is preserved onlapping onto deformed GH rocks (Gehrels et al., 2003, 2006a, 2006b). From restored cross sections (Tobgay et al., 2012; Long et al., 2011b), the minimum basin size is ~200–250 km wide (north–south distance) and >7 km thick.

Correlations between the GH, TH and LH sections allow us to propose a stratigraphic architecture of the pre-collisional northern Indian margin in Bhutan. Fig. 11B shows that proximal deposition of Neoproterozoic–early Paleozoic LH units across much of the Greater Indian margin overlaps in time with deposition of more distal GH protoliths, as originally suggested by Jiang et al. (2003). We propose that a thick, latest Cambrian–Ordovician basin existed between the Neoproterozoic to Lower Cambrian shelf (in the south), and the Paleozoic orogen that deformed the Neoproterozoic GH section (in the north). We show the basin tapering northward over the deformed part of the GH section, after interpretations of the Kathmandu section in Nepal (Gehrels et al., 2006a, 2006b). We also speculatively show the basin onlapping onto the Neoproterozoic to Lower Cambrian shelf to the south, although this relationship is not exposed. This southward-tapering section received detritus from both the deforming GH section to the north and the Indian craton. Proximal deposition of late Paleozoic to Mesozoic LH units (rarely preserved as <2 km-thick deposits of Permian diamictite and/or Permian through Mesozoic shales and sandstones) across the majority of the Greater Indian margin overlaps in time with deposition of similar age TH strata on the distal Neotethyan passive margin.

7.3. Implications for the pre-Himalayan northern Indian margin

The oldest rocks exposed in the Himalayan orogen are 1.8–1.9 Ga LH metasedimentary and volcanogenic metasedimentary rocks, which are intruded by granitoids now exposed as orthogneiss bodies interspersed throughout the section (e.g., Kohn et al., 2010; Gehrels et al., 2011). The post-Paleoproterozoic LH section records a more complex history of deposition, with long periods with no preserved rock record (Yin, 2006; Long et al., 2011a; McKenzie et al., 2011). In Nepal and NW India deposition continued through the early Mesoproterozoic (Gehrels et al., 2011; Martin et al., 2011; McKenzie et al., 2011), while in Bhutan the next time period with substantial deposition is the Neoproterozoic. The 0.9 Ga maximum deposition age of the Baxa Group and Jaishidanda Formation in eastern Bhutan defines an unconformity above the Paleoproterozoic Daling Shumar Group that represents ~0.9–1.0 b.y. Based on the maximum deposition age of the Pangsari formation (1250 Ma) in western Bhutan, the unconformity there may only span 0.5–0.6 b.y. This same unconformity is recognized across the Indian Margin but varies in duration. On the Indian Craton and in NW India McKenzie et al. (2011) constrained the unconformity between 1.1 and 1.6 Ga, a duration of 500 m.y.

The continuity in DZ signature and depositional age of GH and TH rocks along the entire Indian margin and between the cratonic successions and Himalayan successions (LH, GH, and TH) in NW India is a strong argument for similar controls on sediment transport and deposition along the entire margin (Myrow et al., 2010; McKenzie et al., 2011). Myrow et al. (2010) suggested that the orogenic belts surrounding the Indian craton at this time focused on sediment dispersal toward the northern Indian margin, where it became well mixed and relatively uniform in DZ spectra as well as apparent

provenance. The counter argument to a uniform margin is the preservation of Neoproterozoic through Cambrian rocks across the orogen. The compilation of Long et al. (2011a) highlights that Neoproterozoic through Cambrian LH strata are preserved only along the eastern (Bhutan and Arunachal) and western (NW India) portions of the margin, which suggests either variable deposition, or variable pre-Permian erosion. We suggest that the lack of Neoproterozoic through Cambrian LH strata in Nepal combined with more pronounced Paleoproterozoic peaks in Cambrian–Neoproterozoic LH DZ spectra than GH and TH spectra from similar age rocks (Fig. 7) (Fig. 3 in Myrow et al., 2010) highlight two significant depositional systems on the east and west sides of the Indian continent. Thus while the predominant transport systems delivering detritus to the Greater Indian margin (GH and TH protoliths) mostly bypassed the Indian craton, on the eastern (LH rocks in Bhutan) and western (LH rocks in NW India) edges of the system, the transport systems from the growing Neoproterozoic–Cambrian orogenic belts crossed the continent (Fig. 9). In Bhutan this Neoproterozoic–Cambrian deposition is preserved as the Baxa Group, and portions of the Jaishidanda Formation. Significant variations in DZ spectra both north to south and east to west across Bhutan argue against significant mixing of detritus and support a source region from the southeast. As described in Section 7.1, the Neoproterozoic–Cambrian component becomes less significant, and in some samples completely lost in Baxa Group rocks in western Bhutan. We suggest that the Baxa Group formed a well-developed, composite carbonate/siliciclastic, Neoproterozoic to Early Cambrian platform (Tewari, 2003; Tewari and Sial, 2007), similar to what is interpreted for the Krol through Tal Formations of NW India (e.g., Jiang et al., 2003).

There is a growing body of evidence supporting early Paleozoic deformation, uplift and erosion in the Himalaya (e.g. Gehrels et al., 2003, 2006a, 2006b). Widespread Cambrian–Ordovician metamorphism and igneous activity within the GH section have been linked to uplift, exhumation and deposition of coarse-clastic strata in the TH section (Garzanti et al., 1986; Gehrels et al., 2003, 2006a, 2006b). Erosion was apparently significant enough to unroof late Cambrian–Ordovician plutons in the GH section, which contributed a significant proportion of the detritus observed in synorogenic Ordovician strata (Gehrels et al., 2006a, 2006b). These conglomerate sections have been recognized both north (Garzanti et al., 1986; Myrow et al., 2006) and south (Gehrels et al., 2003, 2006a, 2006b; Long and McQuarrie, 2010) of the GH rocks that preserve the Cambrian–Ordovician metamorphism and igneous activity. Ordovician TH coarse-clastic strata in NW India were initially interpreted as foreland basin deposits to the south of a south-vergent fold-thrust belt (e.g., Garzanti et al., 1986) even though paleocurrent data indicate north directed sediment transport (e.g., Myrow et al., 2006).

The distribution of Ordovician age rocks along the east–west extent of the Himalaya provides insight into the extent of the proposed late Cambrian–Ordovician orogeny as well as the source of the Ordovician sediments. We propose that the Bhutan Himalaya preserves the frontal portion of the southward-tapering Cambrian–Ordovician foreland basin. Imbricated pebble conglomerates show south directed transport of detritus (Fig. 10). Farther to the west in central Nepal, the portion of the preserved foreland basin is the proximal portion of the basin that onlaps onto the part of the GH section that was deformed in the Cambrian–Ordovician event (Gehrels et al., 2003, 2006a, 2006b). The more distal foredeep, which we describe in Bhutan, is not preserved in Nepal. In NW India the Ordovician TH conglomerates are observed north of the deformed GH section, and record north directed transport. GH Cambrian–Ordovician orthogneiss bodies are present 100 + km to the south in the proximal hanging wall of the MCT (Myrow et al., 2006; Spencer et al., 2012), and the Ordovician basin is only present to the north of the STDS. Ordovician channels carved into undeformed Cambrian strata in the Spiti region (Myrow et al., 2006) require that the Cambrian–Ordovician deformation was south of the preserved Ordovician conglomerates, compatible with the north directed paleocurrents measured there (Fig. 9A).

7.4. Implications for stratigraphic basin control on Himalayan structures

Although the Cambrian–Ordovician orogen does not necessarily represent a suture between GH and LH rocks, it exerted a first-order control on the location of the MCT, and possibly the location of potential rifting of the northern Indian margin in the Cretaceous (e.g., van Hinsbergen et al., 2012). Even with this broad control, the MCT cuts obliquely through the late Cambrian–Ordovician orogen, so that in Bhutan the MCT carries a large portion of the foreland basin and a limited thickness of Neoproterozoic strata, in central Nepal the frontal MCT hanging wall coincides with the southern limit of Ordovician thrusting, and in NW India the MCT carries a more northern portion of the late Cambrian–Ordovician orogenic system (Fig. 9). An important conclusion drawn from this relationship is that neither the MCT nor the STD contains the same ages of rocks in their hanging walls or footwalls. For example, if the definition of the TH zone is all rocks north of and structurally above the STDS, then there are no Neoproterozoic–early Cambrian Tethyan rocks in Bhutan. However, at the longitude of Nepal, both the MCT and the STD carry Neoproterozoic rocks.

The variation in age and provenance of rocks carried by major structures highlights the need for both tectonostratigraphic nomenclature that defines specific zones of the Himalayan orogen (TH, GH, LH) with respect to large scale structures, due to the first-order control that these structures have on metamorphic grade, as well as stratigraphic nomenclature that reflects the age, provenance and original depositional environment of the rocks rather than structural position.

8. Conclusions

1. Although the use of DZ and geochemical data have been influential in defining and identifying both provenance and age of stratigraphic units throughout the Himalaya, our data emphasize that DZ spectra are not necessarily homogeneous within a given stratigraphic unit and that the youngest zircons could be dramatically different from the deposition age of the strata that contain them.
2. We show that the Neoproterozoic through the early Cambrian and Ordovician are important periods of deposition along the northeastern Indian margin and are present in Tethyan, Greater, and Lesser Himalayan strata. We suggest that LH strata of this age are not continuous along the margin, but rather their location is a function of major drainage systems that crossed the Indian continent.
3. Neoproterozoic through early Cambrian deposition of Lesser Himalayan rocks is preserved in the Baxa Group. These rocks were the most proximal to the Indian continent. Baxa Group rocks in eastern Bhutan have a ubiquitous Early Neoproterozoic source (1.0 Ga) and a significant early Cambrian source (~520 Ma). Baxa Group samples in western Bhutan all have Paleoproterozoic grains (1.9–1.7 Ga) and only the most proximal samples to India display a young ~500 Ma detrital component.
4. Neoproterozoic through early Cambrian Greater Himalayan sedimentary protoliths are preserved only in the lower metasedimentary unit of this tectonostratigraphic zone in Bhutan.
5. We interpret the abundance of late Cambrian–Ordovician DZ grains in Tethyan Himalayan rocks and in the upper metasedimentary unit of the Greater Himalayan section of Bhutan, the stratigraphic thickness of these rocks, the proximal nature of the deposits (quartz-pebble conglomerates), and the thinning of age-equivalent units to the south as important characteristics that define a retro-arc foreland basin. The southernmost extent of this late Cambrian–Ordovician basin is preserved in the Lesser Himalayan Jaishidanda Formation.
6. We suggest that while Late Cambrian–Ordovician deformation and deposition exerted a first-order control over the location of the future MCT, the position of the MCT relative to the Paleozoic deformation system varies along the Himalayan arc. In Bhutan it carries a significant portion of the Paleozoic foreland basin system, while in Nepal

and northwest India it carries a more internal portion of the Paleozoic orogenic system.

Supplementary data to this article can be found online at http://dx.doi.org/10.1016/j.gr.2012.09.002.

Acknowledgments

We would like to thank Dorji Wangda (the late, former Director General), Department of Geology and Mines and Ugyen Wangda (Head/Chief Geologist), Geological Survey of Bhutan for their assistance and support in Bhutan. Mark Pecha and Nicky Geisler of the Arizona LaserChron Center (supported by EAR-0443387 and EAR-0732436) provided assistance with U–Pb dating and sample preparation, while Nathan Mathabane and Mike Eddy helped analyze samples. We are grateful to Peggy Higgins of the SIREAL lab at the University of Rochester for assistance with $\delta^{13}C$ and $\delta^{18}O$ analyses. This research was supported by EAR-0738522 and a fellowship from the Alexander von Humboldt Foundation (to McQuarrie). Comments and discussions with Aaron Martin and Chris Spencer and reviews by Paul Myrow, Alex Webb, and two anonymous reviewers greatly improved the manuscript.

References

Acharyya, S.K., 1974. Stratigraphy and sedimentation of the Buxa Group, eastern Himalaya. Himalayan Geology 4, 102–116.
Allan, J.R., Matthews, R.K., 1982. Isotope signatures associated with early meteoric diagenesis. Sedimentology 29, 797–817 http://dx.doi.org/10.1111/j.1365-3091.1982.tb00085.x.
Ameen, S.M.M., Wilde, S.A., Kabir, M.Z., Akon, E., Chowdhury, K.R., Khan, M.S.H., 2007. Paleo-proterozoic granitoids in the basement of Bangladesh: a piece of the Indian shield or an exotic fragment of the Gondwana jigsaw? Precambrian Research 12, 380–387.
Bartley, J.K., Kah, L.C., 2004. Marine carbon reservoir, Corg-Ccarb coupling, and the evolution of the Proterozoic carbon cycle. Geology 32, 129–132.
Bartley, J.K., Semikhatov, M.A., Kaufman, A.J., Knoll, A.H., Pope, M.C., Jacobsen, S.B., 2001. Global events across the Mesoproterozoic–Neoproterozoic boundary. C and Sr isotopic evidence from Siberia. Precambrian Research 111, 165–202.
Bhargava, O.N., 1995. The Bhutan Himalaya. A geological account. Calcutta. Geological Society of India Special Publication 39 245 pp.
Bhattacharyya, K., Mitra, G., 2009. A new kinematic evolutionary model for the growth of a duplex—an example from the Rangit duplex, Sikkim Himalaya, India. Gondwana Research 16, 697–715 http://dx.doi.org/10.1016/j.gr.2009.07.006.
Brookfield, M.E., 1993. The Himalayan passive margin from Precambrian to Cretaceous times. Sedimentary Geology 84, 1–35 http://dx.doi.org/10.1016/0037-0738 (93) 90042-4.
Burchfiel, B.C., Zhiliang, C., Hodges, K.V., Yuping, L., Royden, L.H., Changrong, D., Jiene, X., 1992. The south Tibetan detachment system, Himalayan orogen: extension contemporaneous with and parallel to shortening in a collisional mountain belt. Geological Society of America, Special Paper 269 41 pp.
Cawood, P.A., 2005. Terra Australis orogen; Rodinia breakup and development of the Pacific and Iapetus margins of Gondwana during the Neoproterozoic and Paleozoic. Earth-Science Reviews 69, 249–279 http://dx.doi.org/10.1016/j.earscirev.2004.09.001.
Cawood, P.A., Buchan, C., 2007. Linking accretionary orogenesis with supercontinent assembly. Earth-Science Reviews 82, 217–256 http://dx.doi.org/10.1016/j.earscirev.2007.03.003.
Cawood, P.A., Korsch, R.J., 2008. Assembling Australia: Proterozoic building of a continent. Precambrian Research 166, 1–35 http://dx.doi.org/10.1016/j.precamres.2008.08.006.
Cawood, P.A., Johnson, M.R.W., Nemchin, A.A., 2007. Early Paleozoic orogenesis along the Indian margin of Gondwana: tectonic response to Gondwana assembly. Earth and Planetary Science Letters 255, 70–84 http://dx.doi.org/10.1016/j.epsl.2006.12.006.
Chakungal, J., Dostal, J., Grujic, D., Duchêne, S., Ghalley, K.S., 2010. Provenance of the Greater Himalayan Sequence: evidence from mafic granulites and amphibolites in NW Bhutan. Tectonophysics 480, 198–212.
Chatterjee, N., Mazumdar, A.C., Bhattacharya, A., Saikia, R.R., 2007. Mesoproterozoic granulites of the Shillong-Meghalaya Plateau: evidence of westward continuation of the Prydz Bay Pan-African suture into Northeastern India. Precambrian Research 152, 1–26 http://dx.doi.org/10.1016/j.precamres.2006.08.011.
Collins, A.S., Pisarevsky, S.A., 2005. Amalgamating eastern Gondwana: the evolution of the Circum-Indian Orogens. Earth-Science Reviews 71, 229–270.
Corrie, S.L., Kohn, M.J., McQuarrie, N., Long, S.P., 2012. Flattening the Bhutan Himalaya. Earth and Planetary Science Letters 349–350, 67–74 http://dx.doi.org/10.1016/j.epsl.2012.07.001.
Dahlen, F.A., 1990. Critical taper model of fold-and-thrust belts and accretionary wedges. Annual Review of Earth and Planetary Sciences 18, 55–99 http://dx.doi.org/10.1146/annurev.ea.18.050190.000415.
Dahlen, F.A., Suppe, J., 1988. Mechanics, growth, and erosion of mountain belts. In: Clark, S.P., et al. (Ed.), Processes in Continental Lithospheric Deformation: Geological Society of America Special Paper, 218, pp. 161–178.
Davidson, C., Grujic, D.E., Hollister, L.S., Schmid, S.M., 1997. Metamorphic reactions related to decompression and synkinematic intrusion of leucogranite, High Himalayan crystallines, Bhutan. Journal of Metamorphic Geology 15, 593–612 http://dx.doi.org/10.1111/j.1525-1314.1997.00044.x.
Davis, D., Suppe, J., Dahlen, F.A., 1983. Mechanics of fold-thrust belts and accretionary wedges. Journal of Geophysical Research 88, 1153–1172.
DeCelles, P.G., Gehrels, G.E., Quade, J., LaReau, B., Spurlin, M., 2000. Tectonic implications of U–Pb zircon ages of the Himalayan orogenic belt in Nepal. Science 288, 497–499 http://dx.doi.org/10.1126/science.288.5465.497.
DeCelles, P.G., Gehrels, G.E., Najman, Y., Martin, A.J., Carter, A., Garzanti, E., 2004. Detrital geochronology and geochemistry of Cretaceous–early Miocene strata of Nepal: Implications for timing and diachroneity of initial Himalayan orogenesis. Earth and Planetary Science Letters 227, 313–330 http://dx.doi.org/10.1016/j.epsl.2004.08.019.
DeGraaff-Surpless, K., Mahoney, J.B., Wooden, J.L., McWilliams, M.O., 2003. Lithofacies control in detrital zircon provenance studies: insights from the Cretaceous Methow basin, southern Canadian Cordillera. Geological Society of America Bulletin 115, 899–915 http://dx.doi.org/10.1130/B25267.1.
Dickinson, W.R., Gehrels, G.E., 2009. Use of U–Pb ages of detrital zircons to infer maximum depositional ages of strata: a test against a Colorado Plateau Mesozoic database. Earth and Planetary Science Letters 288, 115–125 http://dx.doi.org/10.1016/j.epsl.2009.09.013.
Gansser, A., 1964. Geology of the Himalayas. Wiley-Interscience, New York . 289 pp.
Gansser, A., 1983. Geology of the Bhutan Himalaya. Birkhauser Verlag, Boston . 181 pp.
Garzanti, E., Casnedi, R., Jadoul, F., 1986. Sedimentary evidence of a Cambro-Ordovician orogenic event in the northwestern Himalaya. Sedimentary Geology 48, 237–265 http://dx.doi.org/10.1016/0037-0738(86)90032-1.
Gehrels, G.E., DeCelles, P.G., Martin, A., Ojha, T.P., Pinhassi, G., Upreti, B.N., 2003. Initiation of the Himalayan orogen as an early Paleozoic thin-skinned thrust belt. GSA Today 13, 4–9 http://dx.doi.org/10.1130/1052- 5173(2003) 13<4:IOTHOA>2.0.CO;2.
Gehrels, G.E., DeCelles, P.G., Ojha, T.P., Upreti, B.N., 2006a. Geologic and U–Th–Pb geochronologic evidence for early Paleozoic tectonism in the Kathmandu thrust sheet, central Nepal Himalaya. Geological Society of America Bulletin 118, 185–198 http://dx.doi.org/10.1130/B25753.1.
Gehrels, G.E., Valencia, V., Pullen, A., 2006b. Detrital zircon geochronology by Laser–Ablation Multicollector ICPMS at the Arizona LaserChron Center. In: Olszewski, T., Huff, W. (Eds.), Geochronology: Emerging Opportunities, Paleontological Society Short Course, October 21, 2006, Philadelphia, PA: Paleontological Society Paper, 12, pp. 1–10.
Gehrels, G.E., Valencia, V., Ruiz, J., 2008. Enhanced precision, accuracy, efficiency, and spatial resolution of U–Pb ages by laser ablation–multicollector–inductively coupled plasma–mass spectrometry. Geochemistry, Geophysics, Geosystems 9, Q03017 http://dx.doi.org/10.1029/2007GC001805.
Gehrels, G.E., Kapp, P., DeCelles, P.G., Pullen, A., Blakey, R., Weislogel, A., Ding, L., Guynn, J., Martin, A., McQuarrie, N., Yin, A., 2011. Detrital zircon geochronology of pre-Tertiary strata in the Tibetan-Himalayan orogeny. Tectonics 30, TC5016 http://dx.doi.org/10.1029/2011TC002868.
Grujic, D., Hollister, L.S., Parrish, R.R., 2002. Himalayan metamorphic sequence as an orogenic channel: insight from Bhutan. Earth and Planetary Science Letters 98, 177–191 http://dx.doi.org/10.1016/S0012-821X(02)00482-X.
Guerrera Jr., A., Peacock, S.M., Knauth, L.P., 1997. Large 18O and 13C depletions in greenschist facies carbonate rocks, western Arizona. Geology 25, 943–946 http://dx.doi.org/10.1130/0091-7613(1997)025<0943:LOACDI>2.3.CO;2.
Guillot, S., Garzanti, E., Baratoux, D., Marquer, D., Mahéo, G., de Sigoyer, J., 2003. Reconstructing the total shortening history of the NW Himalaya. Geochemistry, Geophysics, Geosystems 4, 1064 http://dx.doi.org/10.1029/2002GC000484.
Halverson, G.P., Hoffman, P.F., Schrag, D.P., Maloof, A.C., Rice, A.H.N., 2005. Towards a Neoproterozoic composite carbon-isotope record. Geological Society of America Bulletin 117, 1181–1207.
Hayden, H.H., 1904. The geology of Spiti, with parts of Bashahr and Rupshu. Geological Survey of India Memoir 36, 1–129.
Heim, A., Gansser, A., 1939. Central Himalaya: geological observations of the Swiss expedition, 1936. Memoirs of the Swiss Society of Natural Sciences 73 245 pp.
Hodges, K.V., 2000. Tectonics of the Himalaya and southern Tibet from two perspectives. Geological Society of America Bulletin 112, 324–350 http://dx.doi.org/10.1130/0016-7606(2000) 112<324:TOTHAS>2.0.CO;2.
Hughes, N.C., Myrow, P.M., McKenzie, N.R., Harper, D.A.T., Bhargava, O.N., Tangri, S.K., Ghalley, K.S., Fanning, C.M., 2010. Cambrian rocks and faunas of the Wachi La, Black Mountains, Bhutan. Geological Magazine 29 http://dx.doi.org/10.1017/S0016756810000750.
Imayama, T., Arita, K., 2008. Nd isotopic data reveal the material and tectonic nature of the Main Central Thrust zone in Nepal Himalaya. Tectonophysics 451, 265–281 http://dx.doi.org/10.1016/j.tecto.2007.11.051.
Jacobsen, S.B., Kaufman, A.J., 1999. The Sr, C, and O isotopic evolution of Neoproterozoic seawater. Chemical Geology 161, 37–57 http://dx.doi.org/10.1016/S0009-2541(99) 00080-7.
Jiang, G., Christie-Blick, N., Kaufman, A.J., Banerjee, D.M., Rai, V., 2003. Carbonate platform growth and cyclicity at a terminal Proterozoic passive margin, Infra Krol Formation and Krol Group, Lesser Himalaya, India. Sedimentology 50, 921–952 http://dx.doi.org/10.1046/j.1365-3091.2003.00589.x.
Joshi, A., 1989. Marine Permian fossils from the foothills of the Bhutan Himalaya. Current Science 59, 318–321.
Kah, L.C., Sherman, A.B., Narbonne, G.M., Kaufman, A.J., Knoll, A.H., James, N.P., 1999. Isotope stratigraphy of the Mesoproterozoic Bylot Supergroup, Northern Baffin

Island: implications for regional lithostratigraphic correlations. Canadian Journal of Earth Sciences 36, 313–332.
Kaufman, A.J., Knoll, A.H., 1995. Neoproterozoic variations in the C-isotopic composition of seawater: stratigraphic and biogeochemical implications. Precambrian Research 73, 27–49 http://dx.doi.org/10.1016/0301-9268(94)00070-8.
Kaufman, A.J., Jiang, G., Christie-Blick, N., Banerjee, D.M., Rai, V., 2006. Stable isotope record of the terminal Neoproterozoic Krol platform in the Lesser Himalayas of northern India. Precambrian Research 147, 156–185.
Kaufman, A.J., Corsetti, F.A., Varni, M.A., 2007. The effect of rising atmospheric oxygen on carbon and sulfur isotope anomalies in the Neoproterozoic Johnnie Formation, Death Valley, USA. Chemical Geology 237, 47–63.
Klootwijk, C.T., Gee, J.S., Pierce, J.W., Smith, G.M., Macfadden, P.L., 1992. An early India–Asia contact: paleomagnetic constraints from Ninetyeast Ridge, ODP Leg 121. Geology 20, 395–398.
Knauth, L.P., Kennedy, M.J., 2009. The late Precambrian greening of the Earth. Nature 460, 728–732.
Kohn, M.J., 2008. P-T-t data from central Nepal support critical taper and repudiate large-scale channel flow of the Greater Himalayan Sequence. Geological Society of America Bulletin 120, 259–273 http://dx.doi.org/10.1130/B26252.1.
Kohn, M.J., Pau, S.K., Corrie, S.L., 2010. The lower Lesser Himalayan sequence: a Paleoproterozoic arc on the northern margin of the Indian plate. Geological Society of America Bulletin 122, 323–335 http://dx.doi.org/10.1130/B26587.1.
Leech, M.L., Singh, S., Jain, A.K., Klemperer, S.L., Manickavasagam, R.M., 2005. The onset of India–Asia continental collision: Early, steep subduction required by the timing of UHP metamorphism in the western Himalaya. Earth and Planetary Science Letters 234, 83–97 http://dx.doi.org/10.1016/j.epsl.2005.02.038.
LeFort, P., 1975. Himalayas: the collided range. Present knowledge of the continental arc. American Journal of Science 275–A, 1–44.
Lohmann, K.C., 1988. Geochemical patterns of meteoric diagenetic systems and their application to studies of paleokarst. In: James, N.P., Choquette, P.W. (Eds.), Paleokarst. Springer-Verlag, Berlin, pp. 50–80.
Long, S., McQuarrie, N., 2010. Placing limits on channel flow: insights from the Bhutan Himalaya. Earth and Planetary Science Letters 290, 375–390 http://dx.doi.org/10.1016/j.epsl.2009.12.033.
Long, S., McQuarrie, N., Tobgay, T., Rose, C., Gehrels, G., Grujic, D., 2011a. Tectonostratigraphy of the Lesser Himalaya of Bhutan: implications for the along-strike stratigraphic continuity of the northern Indian margin. Geological Society of America Bulletin http://dx.doi.org/10.1130/B30202.1.
Long, S., McQuarrie, N., Tobgay, T., Grujic, D., 2011b. Geometry and crustal shortening of the Himalayan fold-thrust belt, eastern and central Bhutan. Geological Society of America Bulletin http://dx.doi.org/10.1130/B30203.1.
Long, S., McQuarrie, N., Tobgay, T., Hawthorne, J., 2011c. Quantifying internal strain and deformation temperature in the eastern Himalaya: implications for the evolution of strain in thrust sheets. Journal of Structural Geology 32, 579–608 http://dx.doi.org/10.1016/j.jsg.2010.12.011.
Long, S.P., McQuarrie, N., Tobgay, T., Grujic, D., Hollister, L., 2011c. Geologic map of Bhutan: The Journal of Maps 2011, 184–192, 1:500,000-scale. doi:10.4113/jom.2011.1159.
Mallett, F.R., 1875. On the geology and mineral resources of Darjeeling district and Western Duars. Memoirs of the Geological Survey of India 11, 1–50.
Maloof, A.C., Schrag, D.P., Crowley, J.L., Bowring, S.A., 2005. An expanded record of Early Cambrian carbon cycling from the Anti-Atlas margin, Morocco. Canadian Journal of Earth Sciences 42, 2195–2216 http://dx.doi.org/10.1139/E05-062.
Maloof, A.C., Ramezani, J., Bowring, S.A., Fike, D.A., Porter, S.M., Mazouad, M., 2010. Constraints on early Cambrian carbon cycling from the duration of the Nemakit-Daldynian–Tommotian boundary $\delta^{13}C$ shift. Morocco, Geology 38, 623–626 http://dx.doi.org/10.1130/G30726.1.
Martin, A.J., DeCelles, P.G., Gehrels, G.E., Patchett, P.J., Isachsen, C., 2005. Isotopic and structural constraints on the location of the Main Central thrust in the Annapurna Range, central Nepal Himalaya. Geological Society of America Bulletin 117, 926–944 http://dx.doi.org/10.1130/B25646.1.
Martin, A.J., Burgy, K.D., Kaufman, A.J., Gehrels, G.E., 2011. Stratigraphic and tectonic implications of field and isotopic constraints on depositional ages of Proterozoic Lesser Himalayan rocks in central Nepal. Precambrian Research 185, 1–17 http://dx.doi.org/10.1016/j.precamres.2010. 11.003.
McKenzie, N.R., Hughes, N.C., Myrow, P.M., Xiao, S., Sharma, M., 2011. Correlation of Precambrian–Cambrian sedimentary successions across northern India and the utility of isotopic signatures of Himalayan lithotectonic zones. Earth and Planetary Science Letters 213, 471–483 http://dx.doi.org/10.1016/j.epsl.2011.10.027.
McQuarrie, N., 2004. Crustal-scale geometry of Zagros fold-thrust belt, Iran. Journal of Structural Geology 26, 519–535.
McQuarrie, N., Robinson, D., Long, S., Tobgay, T., Grujic, D., Gehrels, G., Ducea, M., 2008. Preliminary stratigraphic and structural architecture of Bhutan: implications for the along-strike architecture of the Himalayan system. Earth and Planetary Science Letters 272, 105–117 http://dx.doi.org/10.1016/j.epsl.2008.04.030.
Meert, J.G., 2003. A synopsis of events related to the assembly of eastern Gondwana. Tectonophysics 362, 1–40 http://dx.doi.org/10.1016/S0040-1951(02)00629-7.
Melezhik, V.A., Fallick, A.E., Smirnov, Y.P., Yaklovlev, Y.N., 2003. Fractionation of carbon and oxygen isotopes in 13C-rich Paleoproterozoic dolostones in the transition from medium-grade to high-grade green-schist facies: a case study from the Kola superdeep drillhole. Journal of the Geological Society of London 160, 71–82 http://dx.doi.org/10.1144/0016-764902-008.
Mitra, G., 1994. Strain variation in thrust sheets and across the Sevier fold-and-thrust belt (Idaho–Utah–Wyoming). Implications for section restoration and wedge taper evolution. Journal of Structural Geology 16, 585–602.
Mitra, G., Bhattacharyya, K., Mukul, M., 2010. The Lesser Himalayan duplex in Sikkim: implications for variations in Himalayan shortening. Journal of the Geological Society of India 75, 276–288 http://dx.doi.org/10.1007/s12594-010-0016-x.
Myrow, P.M., Hughes, N.C., Paulsen, T., Williams, I., Parcha, S.K., Thompson, K.R., Bowring, S.A., Peng, S.-C., Ahluwalia, A.D., 2003. Integrated tectonostratigraphic analysis of the Himalaya and implications for its tectonic reconstruction. Earth and Planetary Science Letters 212, 433–441 http://dx.doi.org/10.1016/S0012-821X(03)00280-2.
Myrow, P.M., Thompson, K.R., Hughes, N.C., Paulsen, T.S., Sell, B.K., Parcha, S.K., 2006. Cambrian stratigraphy and depositional history of the northern Indian Himalaya, Spiti Valley, north-central India. Geological Society of America Bulletin 118, 491–510 http://dx.doi.org/10.1130/B25828.1.
Myrow, P.M., Hughes, N.C., Searle, M.P., Fanning, C.M., Peng, S.-C., Parcha, S.K., 2009. Stratigraphic correlation of Cambrian-Ordovician deposits along the Himalaya: Implications for the age and nature of rocks in the Mount Everest region. Geological Society of America Bulletin 121, 323–332 http://dx.doi.org/10.1130/B26384.1.
Myrow, P.M., Hughes, N.C., Goodge, J.W., Fanning, C.M., Williams, I.S., Peng, S., Bhargava, O.N., Parcha, S.K., Pogue, K.R., 2010. Extraordinary transport and mixing of sediment across Himalayan central Gondwana during the Cambrian–Ordovician. Geological Society of America Bulletin 122, 1660–1670 http://dx.doi.org/10.1130/B30123.1.
Otamendi, J.E., Ducea, M.N., Tibaldi, A.M., Bergantz, G.W., de la Rosa, J.D., Vujovich, G.I., 2009. Generation of tonalitic and dioritic magmas by coupled partial melting of gabbroic and metasedimentary rocks within the deep crust of the Famatinian magmatic arc, Argentina. Journal of Petrology 50, 841–873 http://dx.doi.org/10.1093/petrology/egp022.
Parrish, R.R., Hodges, K.V., 1996. Isotopic constraints on the age and provenance of the Lesser and Greater Himalayan sequences, Nepalese Himalaya. Geological Society of America Bulletin 108, 904–911 http://dx.doi.org/10.1130/0016-7606(1996)108<0904:ICOTAA>2.3.CO;2.
Richards, A., Parrish, R., Harris, N., Argles, T., Zhang, L., 2006. Correlation of Lithotectonic units across the eastern Himalaya, Bhutan. Geology 34, 341–344 http://dx.doi.org/10.1130/G22169.1.
Robinson, D.M., DeCelles, P.G., Patchett, P.J., Garzione, C.N., 2001. The kinematic evolution of the Nepalese Himalaya interpreted from Nd isotopes. Earth and Planetary Science Letters 192, 507–521.
Rowley, D., 1996. Age of initiation of collision between India and Asia: a review of stratigraphic data. Earth and Planetary Science Letters 145, 1–13.
Saltzman, M.R., 2005. Phosphorous, nitrogen, and the redox evolution of the Paleozoic oceans. Geology 33, 573–576 http://dx.doi.org/10.1130/G21535.1.
Sengupta, S., Raina, P.L., 1978. Geology of parts of the Bhutan foothills adjacent to Darjeeling district. Indian Journal of Earth Sciences 5, 20–23.
Spencer, C.J., Harris, R.A., Dorais, M.J., 2012. Depositional provenance of the Himalayan metamorphic core of Garhwal region, India: Constrained by U–Pb and Hf isotopes in zircons. Gondwana Research http://dx.doi.org/10.1016/j.gr.2011.10.004.
Swapp, S.M., Hollister, L.S., 1991. Inverted metamorphism within the Tibetan slab of Bhutan: evidence for a tectonically transported heat source. The Canadian Mineralogist 29, 1019–1041.
Tangri, S.K., 1995. Baxa Group. In: Bhargava, O.N. (Ed.), The Bhutan Himalaya: A Geological Account: Geological Society of India Special Publication, 39, pp. 38–58.
Tangri, S.K., Pande, A.C., 1995. Tethyan sequence. In: Bhargava, O.N. (Ed.), The Bhutan Himalaya: A Geological Account: Geological Society of India Special Publication, 39, pp. 109–142.
Tewari, V.C., 2003. Sedimentology, palaeobiology and stable isotope chemostratigraphy of the Terminal Neoproterozoic Buxa Dolomite, Arunachal Pradesh NE Lesser Himalaya. Journal of Himalayan Geology 24, 1–18.
Tewari, V.C., Sial, A.N., 2007. Neoproterozoic–Early Cambrian isotopic variation and chemostratigraphy of the Lesser Himalaya, India Eastern Gondwana. Chemical Geology 237, 64–88 http://dx.doi.org/10.1016/j.chemgeo.2006.06.015.
Tobgay, T., Long, S.P., McQuarrie, N., Ducea, M., Gehrels, G., 2010. Using isotopic and chronologic data to fingerprint strata: the challenges and benefits of variable sources to tectonic interpretations, the Paro Formation, Bhutan Himalaya. Tectonics 29, TC6023 http://dx.doi.org/10.1029/2009TC002637.
Tobgay, T., McQuarrie, N., Long, S., Kohn, M., Corrie, S., 2012. The age and rate of displacement along the Main Central thrust in the western Bhutan Himalaya. Earth and Planetary Science Letters 319–320, 146–158 http://dx.doi.org/10.1016/j.epsl.2011.12.005.
Valdiya, K.S., 1995. Proterozoic sedimentation and Pan-African geodynamic development in the Himalaya. Precambrian Research 74, 35–55 http://dx.doi.org/10.1016/0301-9268(95)00004-O.
Van Hinsbergen, D.J.J., Lippert, P.C., Dupont-Nivet, G., McQuarrie, N., Doubrovine, P.V., Sakman, W., Torsvink, T.H., 2012. Greater India Basin hypothesis and a two-stage Cenozoic collision between India and Asia. Proceedings of the National Academy of Science http://dx.doi.org/10.1073/pnas.1117262109.
Webb, A.A.G., Yin, A., Harrison, T.M., Celerier, J., Burgess, P.W., 2007. The leading edge of the Greater Himalayan crystalline complex revealed in the NW Indian Himalaya: implications for the evolution of the Himalayan orogeny. Geology 35, 955–958 http://dx.doi.org/10.1130/G23931A.1.
Webb, A.A.G., Yin, A., Harrison, T.M., Celerier, J., Gehrels, G.E., Manning, C.E., Grove, M., 2011. Cenozoic tectonic history of the Himachal Himalaya (northwestern India) and its constraints on the formation mechanism of the Himalayan orogen. Geosphere 7, 1013–1061 http://dx.doi.org/10.1130/GES00627.1.
Yin, A., 2006. Cenozoic tectonic evolution of the Himalayan orogen as constrained by along-strike variation of structural geometry, exhumation history, and foreland sedimentation. Earth-Science Reviews 76, 1–131 http://dx.doi.org/10.1016/j.earscirev.2005.05.004.

Yin, A., Dubey, C.S., Kelty, T.K., Webb, A.A.G., Harrison, T.M., Chou, C.Y., Célérier, J., 2010a. Geologic correlation of the Himalayan orogen and Indian craton: Part 1. Structural geology, U–Pb zircon geochronology, and tectonic evolution of the Shillong Plateau and its neighboring regions in NE India. Geological Society of America Bulletin 122, 336–359 http://dx.doi.org/10.1130/B26460.1.

Yin, A., Dubey, C.S., Kelty, T.K., Webb, A.A.G., Harrison, T.M., Chou, C.Y., Celerier, J., 2010b. Geologic Correlation of the Himalayan orogen and Indian craton: Part 2. Structural geology, geochronology, and tectonic evolution of the Eastern Himalaya. Geological Society of America Bulletin 122, 360–395 http://dx.doi.org/10.1130/B26461.1.